ELSEVIER

Chemistry & Biology 8 (2001) 913–929

Chemistry & Biology

www.elsevier.com/locate/chembiol

Research Paper

Extended peptide-based inhibitors efficiently target the proteasome and reveal overlapping specificities of the catalytic β-subunits

Benedikt M. Kessler [a], Domenico Tortorella [a], Mikael Altun [a], Alexei F. Kisselev [b], Edda Fiebiger [a], Brian G. Hekking [a], Hidde L. Ploegh [a,*], Herman S. Overkleeft [a]

[a] *Department of Pathology, Harvard Medical School, 200 Longwood Avenue, Boston, MA 02115, USA*
[b] *Department of Cell Biology, Harvard Medical School, 200 Longwood Avenue, Boston, MA 02115, USA*

Received 18 April 2001; revisions requested 8 June 2001; revisions received 19 June 2001; accepted 26 June 2001
First published online 8 August 2001

Abstract

Background: The 26S proteasome is responsible for most cytosolic proteolysis, and is an important protease in major histocompatibility complex class I-mediated antigen presentation. Constitutively expressed proteasomes from mammalian sources possess three distinct catalytically active species, β1, β2 and β5, which are replaced in the γ-interferon-inducible immunoproteasome by a different set of catalytic subunits, β1i, β2i and β5i, respectively. Based on preferred cleavage of short fluorogenic peptide substrates, activities of the proteasome have been assigned to individual subunits and classified as 'chymotryptic-like' (β5), 'tryptic-like' (β2) and 'peptidyl-glutamyl peptide hydrolyzing' (β1). Studies with protein substrates indicate a far more complicated, less strict cleavage preference. We reasoned that inhibitors of extended size would give insight into the extent of overlapping substrate specificity of the individual activities and subunits.

Results: A new class of proteasome inhibitors, considerably extended in comparison with the commonly used fluorescent substrates and peptide-based inhibitors, has been prepared. Application of the safety catch resin allowed the generation of the target compounds using a solid phase protocol. Evaluation of the new compounds revealed a set of highly potent proteasome inhibitors that target all individual active subunits with comparable affinity, unlike the other inhibitors described to date. Modification of the most active compound, adamantane-acetyl-(6-aminohexanoyl)$_3$-(leucinyl)$_3$-vinyl-(methyl)-sulfone (Ada-Ahx$_3$L$_3$VS), itself capable of proteasome inhibition in living cells, afforded a new set of radio- and affinity labels.

Conclusions: N-terminal extension of peptide vinyl sulfones has a profound influence on both their efficiency and selectivity as proteasome inhibitors. Such extensions greatly enhance inhibition and largely obliterate selectivity towards the individual catalytic activities. We conclude that for the interaction with larger substrates, there appears to be less discrimination of different substrate sequences for the catalytic activities than is normally assumed based on the use of small peptide-based substrates and inhibitors. The compounds described here are readily accessible synthetically, and are more potent inhibitors in living cells than their shorter peptide vinyl sulfone counterparts.

Keywords: Active site label; Inhibitor; Peptide vinyl sulfone; Proteasome; Substrate analog

1. Introduction

The 26S proteasome, a large cytosolic protease complex, is implicated in many biological processes [1–3], including degradation of most cytosolic proteins in mammalian cells and generation of antigenic peptides presented by major histocompatibility complex class I (MHC I) molecules [4,5]. The 26S proteasome is composed of an inner 20S core, with which two 19S caps are associated. The 19S caps contain elements responsible for recognition of ubiquitinated protein substrates and unfolding of substrates targeted to the proteasome in an ATP-dependent manner, whereas the actual proteolytic activity resides in the inner 20S core. In addition to the 19S caps, other multisubunit complexes, such as PA28, modulate proteasome activity. The 20S particle itself consists of 28 individual subunits arranged in cylindrical form of four rings containing seven subunits each. The outer rings, which interact with the 19S regulatory caps, consist of seven highly homologous α-subunits. The two inner rings are assembled from seven distinct β-subunits each, three of which in each ring are

* Corresponding author.
E-mail address: ploegh@hms.harvard.edu (H.L. Ploegh).

1074-5521/01/$ – see front matter
PII: S1074-5521(01)00069-2

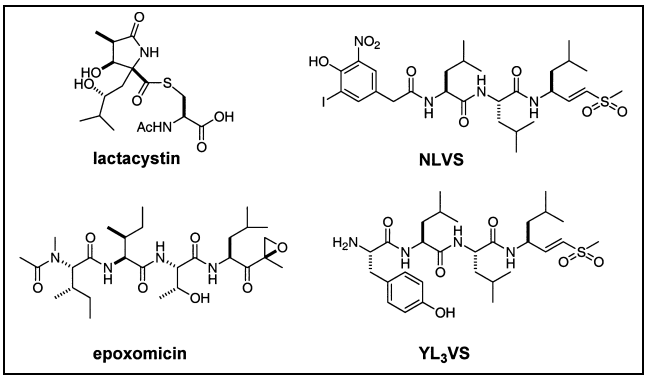

Fig. 1. Proteasome inhibitors. With the exception of lactacystin, proteasome inhibitors are based on small oligopeptide sequences, the C-terminus of which is modified to an electrophilic trap, such as an epoxyketone (epoxomicin) or vinyl sulfone (NLVS, YL_3VS).

catalytically active. In higher vertebrates, these proteolytic β-subunits, β1, β2 and β5, respectively (also referred to as the Y, Z and X subunits), are thought to display three distinct catalytic activities, commonly referred to as the chymotryptic-like activity (attributed to β5), peptidyl-glutamyl peptide hydrolyzing activity (PGPH; β1) and tryptic-like activity (β2). Upon exposure to γ-interferon (IFNγ), antigen presenting cells (APCs) express an additional set of catalytic β-subunits. These subunits, β1i, β2i and β5i (also referred to as LMP2, MECL-1 and LMP7), replace β1, β2 and β5, respectively, to form a new particle, the immunoproteasome [2]. The 19S caps may be replaced by the 11S or PA28 regulatory complex, itself induced by IFNγ.

The precise role of the individual activities in cytosolic proteolysis remains unclear. In a broader sense, this also holds true for our understanding of the immunological necessity for expressing the immunoproteasome to generate antigenic peptides. Whereas an essential role of the immunoproteasome in the generation of suitable oligopeptides for MHC I-mediated antigen presentation is now widely accepted, our understanding of the different substrate specificities of the corresponding catalytic β-subunits for the constitutive proteasome and the immunoproteasome is incomplete. In vitro studies [6,7], in which proteins are exposed to purified 20S proteasomes, followed by analysis of the produced oligopeptides, do not necessarily reflect cleavage patterns that occur in vivo under the influence of the 26S proteasome [8,9]. Current knowledge of both the catalytic mechanism and the substrate specificity of the various catalytic proteasomal β-subunits is based largely on the use of synthetic proteasome inhibitors and artificial, fluorogenic substrates [10]. For several such inhibitors, the structure of the 20S proteasome complex with inhibitor has been solved [11–13]. Indeed, the designation 'chymotryptic-like, PGPH and tryptic-like' hydrolyzing activities, and their assignment to β5, β1 and β2, respectively, is based on proteasomal hydrolysis of fluorogenic substrates [14].

Proteasome inhibitors have proven essential to study proteasome activity in living cells. Well-known proteasome inhibitors include lactacystin [15], epoxomicin [16] as well as the peptide vinyl sulfones NLVS [17] and YL_3VS [18] (Fig. 1). Most proteasome inhibitors, with the fungal metabolite lactacystin as a notable exception, are based on short oligopeptidic sequences, in which the C-terminus (or P1 position) has been replaced with an electrophilic trap, such as an aldehyde [19], a boronate [20] (both of which result in reversible inhibitors), an epoxyketone or a vinyl sulfone [17,18] (generating irreversible inhibitors). Important goals are the development of inhibitors that are subunit-specific and cell-permeable. At the same time, inhibitors that inactivate all β-subunits efficiently and that retain cell permeability would also be useful for both in vitro and in vivo applications. To date, however, none of the available inhibitors targets all β-subunits equally well. Considerable progress in the development of subunit-specific inhibitors has been made by Crews and coworkers, who, by variation of the sequence at P2–P4 in epoxomicin, were able to generate specific inhibitors of the 'chymotryptic-like' [21] and 'PGPH' [22] activities, respectively. Research from our laboratory has shown peptide vinyl sulfones to be potent proteasome inhibitors [17,18]. Based on the trileucine vinyl sulfone core, introduction of different substituents at P4 yielded inhibitors with a preference for β5 (NLVS) and β2 (YL_3VS), respectively, as corroborated by their radiolabeled analogs. More recently, Nazif and Bogyo [23] reported the preparation of a peptide vinyl sulfone library with asparagine vinyl sulfone at P1 that yielded highly specific inhibitors of β2.

The assignment of substrate specificity based on small peptide-based inhibitors, as well as their corresponding substrates, is rather complicated. This is perhaps best illustrated by the fact that the only effective, selective inhibitor of the 'PGPH' activity (sometimes referred to as the 'caspase-like' or 'postacidic' activity depending on the fluorogenic substrate used [24]) in fact contains a leucine epoxyketone moiety (rather than the corresponding glutamate or aspartate derivative) at P1 [22]. We reasoned that it would be desirable to have access to inhibitors which, at least in size, are closer to the natural substrate of the proteasome, that is, presumably, an extended polypeptide chain. Obviously, retention of cell permeability is essential if such inhibitors are to be used in living cells.

Here we report the design and synthesis of a set of novel proteasome inhibitors. The compounds consist of the core trileucine vinyl sulfone moiety and are extended with a number of aminohexanoic acid (Ahx) spacers, followed by N-terminal caps of different size. Ahx spacers were chosen to retain at least some amide linkages, while removing features that might make such extensions cleavable. Even though side chains are obviously absent from these spacers, the spacers themselves as well as their further modification allow the introduction of substantial ad-

ditional mass. A total solid phase synthesis strategy using Kenner's safety catch linker proved to be very suitable for the generation of the target compounds. Characterization of these new proteasome inhibitors showed that the inhibitory properties increased dramatically upon increasing the size of the extensions on the inhibitors. Furthermore, selectivity for individual subunits is largely obliterated upon extension of the inhibitors. These results suggest a higher degree of overlap in specificity between the different catalytic β-subunits of the proteasome than is currently assumed based on the use of small proteasome inhibitors and substrates. The most potent inhibitor of the series proved to be cell-permeable and could be derivatized into a radio- and an affinity label. We demonstrate applications of these compounds in the study of proteasomal function in vitro and in living cells.

2. Results

2.1. Design and synthesis of N-terminally extended proteasome inhibitors

Peptide vinyl sulfones covalently and irreversibly modify the catalytically active β-subunits of the proteasome through a Michael reaction with the hydroxyl moiety of the N-terminal threonine residue. Depending on N-terminal modification, peptides containing the core trileucine vinyl sulfone structure (L_3VS) can target both β2 and β5. Introduction of different substituents at the N-terminus (P4) led to inhibitors with selectivity leaning towards β5/β5i (NLVS, ZL_3VS) or β2/β2i (YL_3VS). We therefore decided to use the L_3VS core as a basis for the generation of new proteasome inhibitors with N-terminal extensions of varied size and composition (Fig. 2).

An obvious approach for the construction of N-terminally extended peptide vinyl sulfones would be elongation with natural amino acids. However, we found that compounds of this type are less desirable as proteasome inhibitors due to their susceptibility to proteasomal cleavage internally (B.M. Kessler and H.L. Ploegh, unpublished results). This observation led us to select 6-Ahx as a suitable linker molecule between the trileucine vinyl sulfone core and different N-terminal caps, such as acetate (Ac), benzyloxycarbonylate (Z) and adamantanylacetate (Ada) substituents. The adamantane moiety was chosen because earlier work with substituted azasugars showed promise for this modification to retain cell permeability [25]. Adamantanylacetic acid was incorporated either as a single residue (as in **5**–**8**, **11**, **12**, **17**) or as a dimer linked through diaminopropionic acid (Dpr, **15**, **16**). Incorporation of tyrosine (Y, **9**–**12**, **14**, **16**) or ε-biotinyl-lysine (K(Bio), **17**) near the N-terminus allowed radiolabeling or streptavidin-mediated detection, respectively, of the modified proteasomal β-subunits.

The target compounds were prepared by either one of

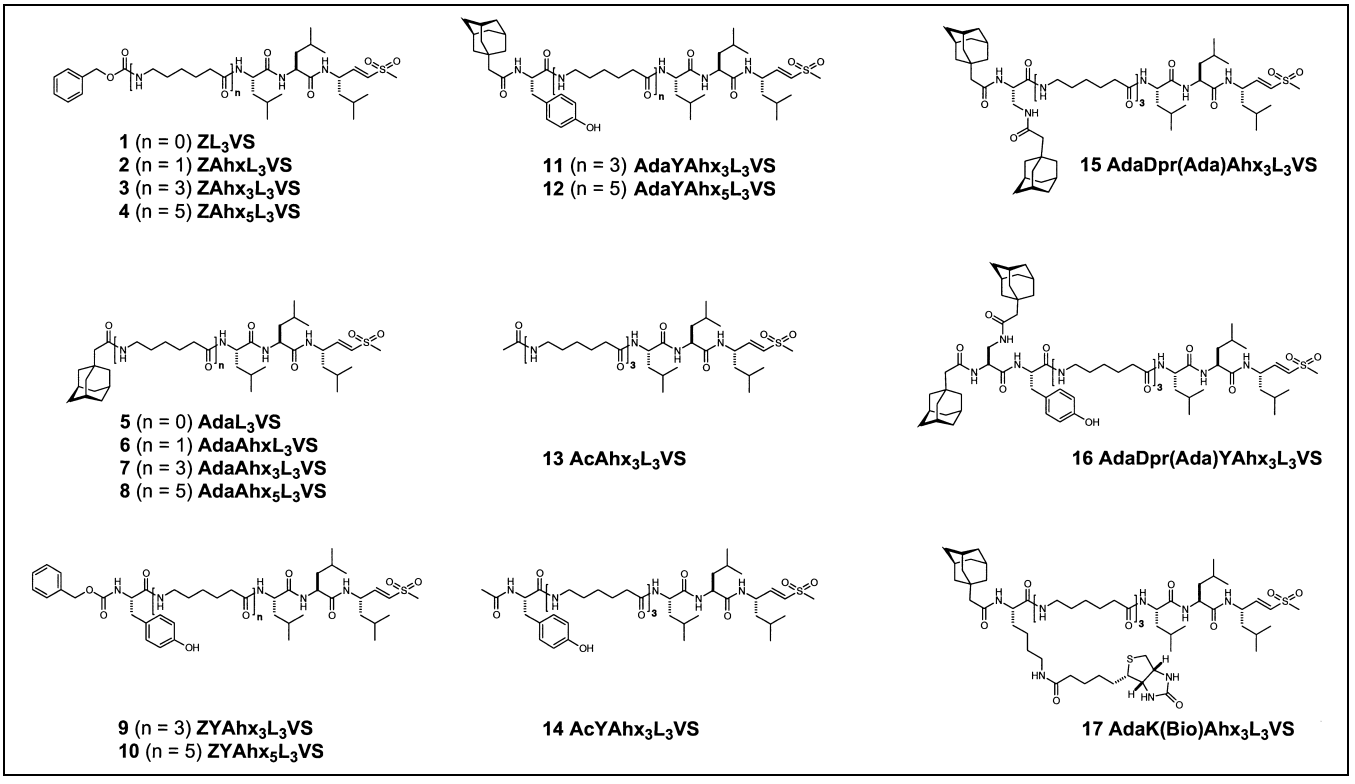

Fig. 2. Design of a new class of substrate-like proteasome inhibitors.

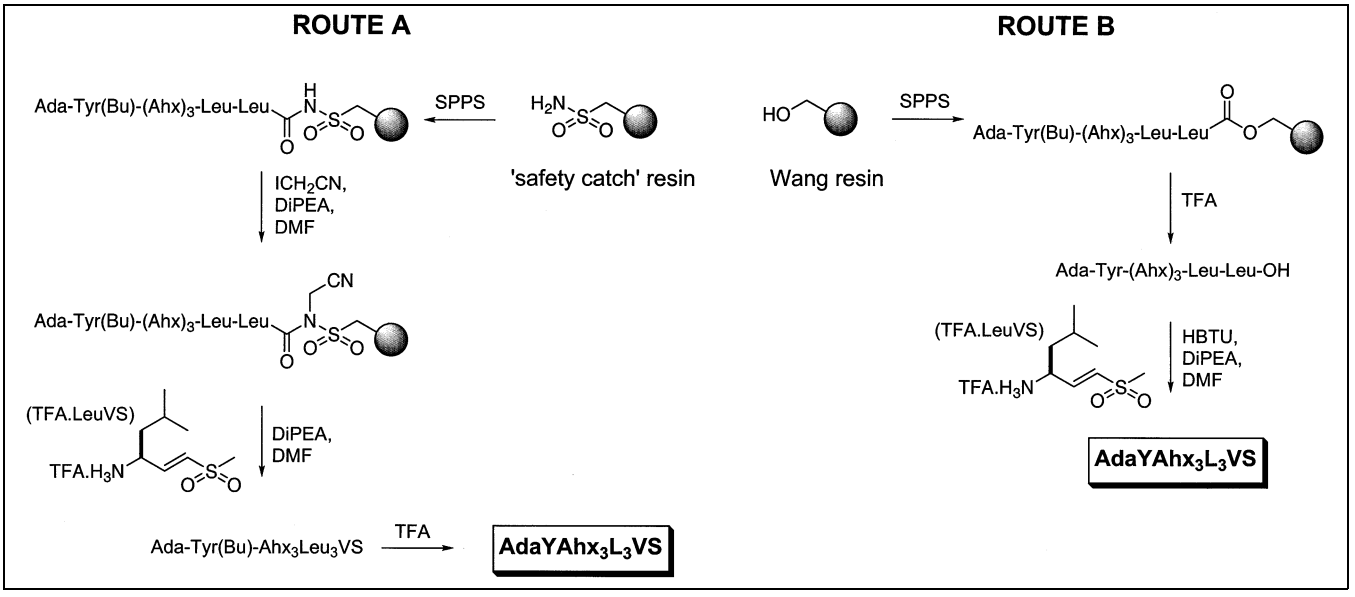

Scheme 1. Synthesis of the proteasome inhibitors. The designed proteasome inhibitors can be prepared using two different synthetic routes. Compounds **1**–**17** were prepared using the safety catch resin, as illustrated for AdaYAhx$_3$L$_3$VS **11** (route A). Alternatively, a conventional block coupling was applied to synthesize compounds **4**, **7**, **11** and **17**, also illustrated for AdaYAhx$_3$L$_3$VS **11** (route B).

two independent synthetic routes (Scheme 1). We recently reported [26] the solid phase synthesis of peptide vinyl sulfone and peptide epoxyketone-based proteasome inhibitors, including ZL$_3$VS **1**. Our strategy is based on the protocols described by Ellman and coworkers [27] who utilized a modification of Kenner's safety catch linker [28] for the synthesis of libraries of fluorogenic peptide substrates [29].

The complete panel of compounds **1**–**17** has been prepared starting from the safety catch resin, as is illustrated for AdaYAhx$_3$L$_3$VS **11** (route A, Scheme 1). 4-Sulfamylbutyrylaminomethyl polystyrene resin (the 'safety catch' resin) was functionalized with Fmoc-leucine following the published procedure [26]. Standard Fmoc-based solid phase peptide synthesis (SPPS) afforded the immobilized protected oligopeptide. Activation of the resin was then accomplished using a 50-fold excess of iodoacetonitrile in the presence of *N*,*N*′-diisopropylethylamine (DiPEA, 10 equivalents) in *N*-methylpyrrolidinone (NMP). Treatment of the activated resin with leucine vinyl sulfone (10 equivalents) and DiPEA (12 equivalents) in dimethyl formamide (DMF, 4 days), and subsequent removal of the *tert*-butyl protective group (trifluoroacetic acid (TFA)/H$_2$O/triisopropylsilane (TIS) 95/2.5/2.5), yielded the target peptide vinyl sulfone, which was purified using reverse phase high performance liquid chromatography (HPLC). Following the safety catch route, the target peptides could be routinely prepared on a 50 μmol scale with purified yields varying from 5 to 30%.

Peptide vinyl sulfones **4**, **7**, **11** and **17** were prepared on a larger scale (0.5–1.0 mmol) following a block coupling protocol [21], as outlined for AdaYAhx$_3$L$_3$VS **11** (route B, Scheme 1). Starting from the Wang resin, SPPS followed by acid-mediated cleavage afforded AdaYAhx$_3$L$_2$OH. Treatment with leucine vinyl sulfone under the agency of *O*-benzotriazol-1-yl-*N*,*N*,*N*′,*N*′-tetramethyluronium hexafluorophosphate (HBTU) and DiPEA in DMF, followed by concentration in vacuo and precipitation from ethyl acetate afforded the target compound **11** in 90% analytical purity. Yields for compounds **4**, **7**, **11** and **17** typically varied from 45 to 50%. Although in theory compounds **1**–**17** are all accessible following the block coupling route, the generation of peptide vinyl sulfones featuring acidic or basic side chain residues through block coupling would obviously require a more elaborate protective group strategy. We find that peptide vinyl sulfones containing such residues as glutamate, lysine or arginine are more conveniently prepared using the safety catch resin (H.S. Overkleeft and H.L. Ploegh, unpublished results).

2.2. *N*-terminal extension dramatically increases proteasome inhibition

As an initial experiment, we assayed the inhibition potency of proteasome inhibitors **1**–**8** (Fig. 3B). Competition experiments were carried out in which we examined the ability of the new proteasome inhibitors to inhibit labeling of proteasomal subunits with ^{125}I-YL$_3$VS (targeting β2/β2i) or ^{125}I-NLVS (targeting β5/β5i). Cell lysates from EL-4 cells, a mouse cell line that expresses both the constitutive proteasome and the immunoproteasome, were incubated with ZL$_3$VS **1**, ZAhxL$_3$VS **2**, ZAhx$_3$L$_3$VS **3**, ZAhx$_5$L$_3$VS **4**, AdaL$_3$VS **5**, AdaAhxL$_3$VS **6**, AdaAhx$_3$L$_3$VS **7** and AdaAhx$_5$L$_3$VS **8**, respectively, at concentrations ranging from 0 to 30 μM. As further controls, we included NLVS, YL$_3$VS and epoxomicin. Resid-

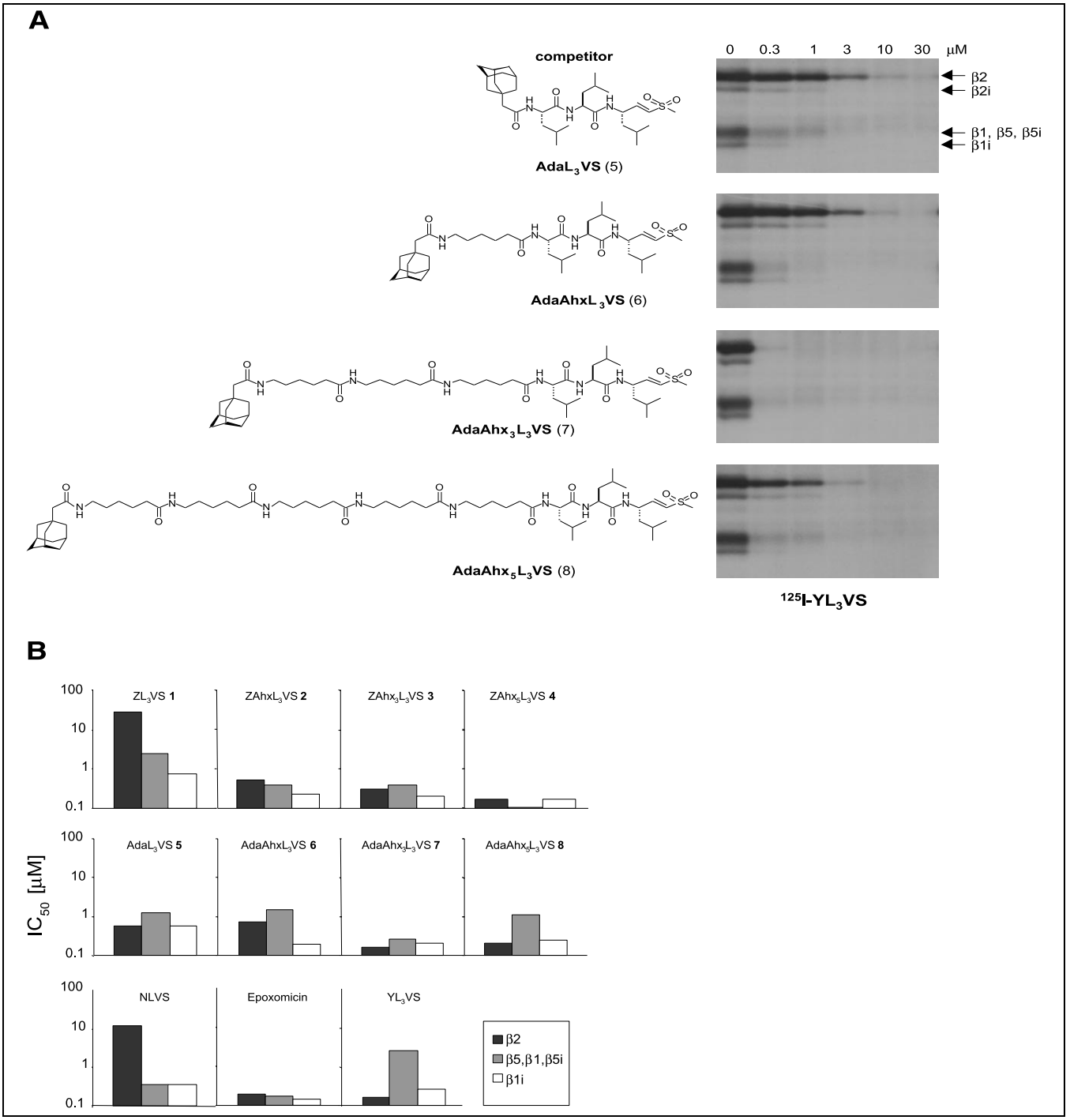

Fig. 3. N-terminal extension influences proteasome inhibition. A: Compounds **5**–**8** were added to EL-4 lysates prior to labeling with ^{125}I-YL$_3$VS. Labeled polypeptides were separated by SDS–PAGE and analyzed by autoradiography; the β1, β5 and β5i polypeptides comigrate in this separation. Inhibition is evident from the disappearance of the labeled proteasomal subunits when test compounds are included. B: IC_{50} values for the concentrations at which compounds **1**–**8**, NLVS, YL$_3$VS and epoxomicin inhibit 50% of labeling of proteasomal subunits by ^{125}I-YL$_3$VS (β2) and ^{125}I-NLVS (β1, β1i, β5, β5i) were determined by densitometry analysis and normalized to 100%.

ual available subunits were labeled by a subsequent incubation with either ^{125}I-YL$_3$VS or ^{125}I-NLVS. Labeled subunits were then resolved by sodium dodecylsulfate–polyacrylamide gel electrophoresis (SDS–PAGE) and autoradiography. The intensity of labeled bands corresponding to relevant subunits (^{125}I-YL$_3$VS-labeled β2, the ^{125}I-NLVS-labeled β5/β5i/β1 polypeptides as well as the ^{125}I-NLVS-labeled β1i) was quantified by densitometry. IC_{50} values (the concentration of inhibitor at which labeling intensity is reduced by 50%) for each compound were calculated (Fig. 3B).

An increase in the number of Ahx residues from zero

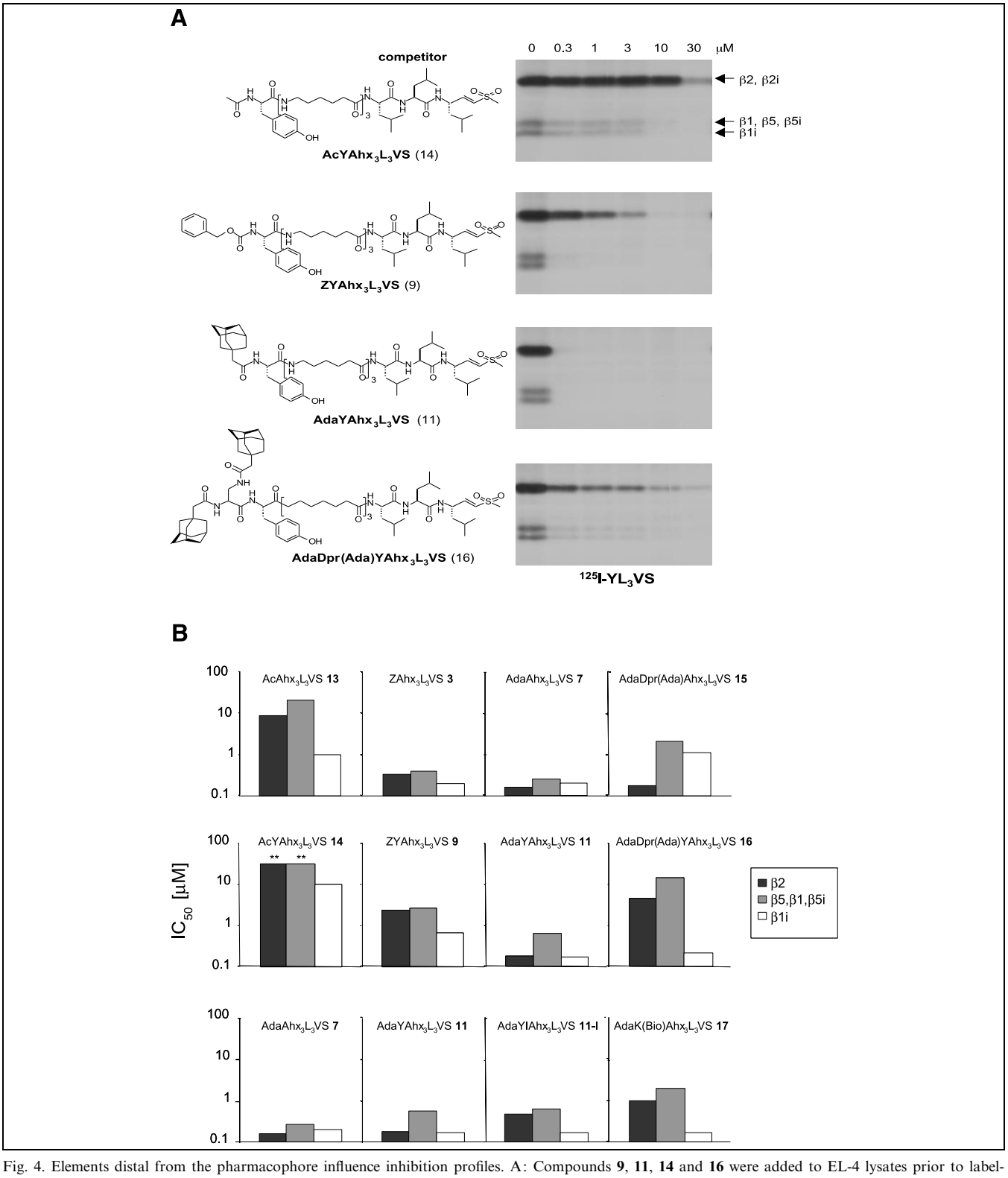

Fig. 4. Elements distal from the pharmacophore influence inhibition profiles. A: Compounds **9**, **11**, **14** and **16** were added to EL-4 lysates prior to labeling with ^{125}I-YL$_3$VS. B: IC$_{50}$ values for the concentrations in which compounds **3**, **7**, **9**, **11**, **11**-I, **13**, **14**, **15**, **16** and **17** inhibit 50% of labeling of proteasomal subunits by ^{125}I-YL$_3$VS (β2, β2i) and ^{125}I-NLVS (β1, β1i, β5, β5i) were determined by densitometry analysis and normalized to 100% (** indicates no inhibition at 30 μM).

(ZL_3VS **1**), to one ($ZAhxL_3VS$ **2**), three ($ZAhx_3L_3VS$ **3**) and five ($ZAhx_5L_3VS$ **4**) dramatically increases inhibition potency, regardless of whether ^{125}I-YL_3VS or ^{125}I-NLVS is used as the label. A loss of subunit specificity thus correlates with increased inhibition. Especially striking is the effect on β2 exerted by $ZAhx_5L_3VS$ **4**: at a concentration as low as 0.3 μM, subsequent labeling of this subunit with ^{125}I-YL_3VS is all but abolished, whereas the parent compound ZL_3VS **1** hardly targets β2 even at a 100-fold higher concentration. We note that the introduction of multiple Ahx spacers does not confer onto these compounds detergent-like properties. In vitro, the 20S proteasome is activated by low concentrations of SDS (0.01%). As a sensitive measure of any detergent-like properties, we compared the effect of 0.01% SDS with that of $AdaAhx_3L_3VS$ on the integrity of EL-4 cells. Whereas 0.01% SDS readily lysed EL-4 cells, as measured by trypan blue exclusion, $AdaAhx_3L_3VS$ **7** at 0.01% w/v (107 μM) did not result in any detectable cell lysis (data not shown). As we shall show below, cells that express a reporter substrate which accumulates in the cytosol upon inactivation of the proteasome likewise retain this cytosolic reporter protein in the presence of $AdaAhx_3L_3VS$ **7**.

A similar trend is observed in the experiments with compounds $AdaAhx_3L_3VS$ **5**–$AdaAhx_5L_3VS$ **8**, containing the more bulky hydrophobic Ada group as the N-terminal cap. However, optimal inhibition is now observed for $AdaAhx_3L_3VS$ **7** (Fig. 3A), with three Ahx residues rather than five, as in $ZAhx_5L_3VS$ **4**. At 0.3 μM of $AdaAhx_3L_3VS$ **7**, labeling with ^{125}I-YL_3VS is largely abolished, $AdaAhx_5L_3VS$ **8** being a weaker inhibitor (Fig. 3). Comparison with known proteasome inhibitors shows that both $ZAhx_5L_3VS$ **4** and $AdaAhx_3L_3VS$ **7** are considerably more potent inhibitors of the proteasome than YL_3VS and NLVS, and are comparable to the natural product epoxomicin.

2.3. *Elements distal from the pharmacophore influence inhibition profiles*

The results described above demonstrate the influence of elements quite distal from P1 on proteasomal inhibition. Although both $ZAhx_3L_3VS$ **3** and $AdaAhx_3L_3VS$ **7** are potent inhibitors, introduction of the Ada moiety at the N-terminus clearly has a beneficial effect when compared with the Z group. We therefore examined the effect of the size of the N-terminal cap in more detail (Fig. 4). EL-4 lysates were treated with $AcAhx_3L_3VS$ **13** and $AdaDpr(Ada)Ahx_3L_3VS$ **15** prior to labeling with either ^{125}I-NLVS or ^{125}I-YL_3VS, in an experiment similar to that described above. Inhibition of labeling was compared with $ZAhx_3L_3VS$ **3** and $AdaAhx_3L_3VS$ **7**, and showed a maximal inhibition for $AdaAhx_3L_3VS$ **7** (Fig. 4B).

To transform the most effective inhibitors into active site probes, a tyrosine residue was incorporated to allow labeling with ^{125}I, and yielded $AcYAhx_3L_3VS$ **14**, $ZYAhx_3L_3VS$ **9**, $AdaYAhx_3L_3VS$ **11** and $AdaDpr(Ada)YAhx_3L_3VS$ **16**. We first examined unlabeled **9**, **11**, **14** and **16** in a competition experiment (Fig. 4A,B). As before, optimal inhibition is achieved when a single Ada (as in **11**) is present at the N-terminus. Comparison between $ZYAhx_5L_3VS$ **10** and $AdaYAhx_5L_3VS$ **12** revealed favorable inhibition properties for the former compound, in line with those observed for compounds **4** and **8** (data not shown). Acetylated compounds **13** and **14** are poor inhibitors (IC_{50} values have dropped below those observed for the small peptide vinyl sulfones ZL_3VS, NLVS and YL_3VS), further underlining the important contributions of distal elements of these inhibitors to proteasomal inhibition. Although not the most potent inhibitors in this series, compounds **15** and **16**, with two bulky Ada groups at the N-terminus, still inactivate the proteasome as efficiently as the standard peptide vinyl sulfones.

2.4. *Generation of novel proteasomal active site labels*

A major advantage of covalent, irreversible proteasome inhibitors, compared to their reversible counterparts, is their ability, through radio- or affinity labeling, to visualize the subunits targeted. Whereas competition experiments using fluorogenic substrates provide at best indirect information on the selectivity of newly designed inhibitors for individual proteasomal subunits, radiolabeled proteasome inhibitors address subunit specificity unambiguously, as demonstrated for [^{3}H]lactacystin [30], and in our laboratory for ^{125}I-NLVS and ^{125}I-YL_3VS [14,15]. Likewise, incorporation of a biotin moiety into the inhibitor allows streptavidin-mediated visualization of the targeted subunits, as exemplified by the biotinylated epoxomicin derivatives reported by Crews and coworkers [31,32].

Incorporation of a tyrosine in close proximity to the N-terminus of the newly designed proteasome inhibitors does not significantly alter inhibitory potency (Fig. 4B, $AdaAhx_3L_3VS$ **7** vs $AdaYAhx_3L_3VS$ **11**). Alternatively, introduction of a phenolic moiety at the C-terminal portion of the inhibitors can be accomplished using leucine vinyl (hydroxyphenyl) sulfone (LeuVS-PhOH) [18] in the synthetic schemes. However, this modification (for instance $ZAhx_5L_3VS$-PhOH compared to $ZAhx_5L_3VS$ **4**) led to a considerable drop in inhibition (data not shown) and was not pursued further. Iodination of the phenol moiety in **11**, as in $AdaY(I)Ahx_3L_3VS$ **11**-I, chemically equivalent to its radioiodinated counterpart, results in the same inhibition profile as that observed for its non-iodinated counterpart. Introduction of a (ε)-biotin-lysine residue, as in $AdaK(Bio)Ahx_3L_3VS$ **17** results in a slight drop of inhibition (Fig. 4B). However, **17** still compares favorably to the smaller peptide vinyl sulfones. Simple replacement of the Ada moiety with biotin, as in $biotinAhx_3L_3VS$, resulted in a steep drop in inhibition (data not shown), underscoring the importance of the Ada moiety at this position distal from the pharmacophore.

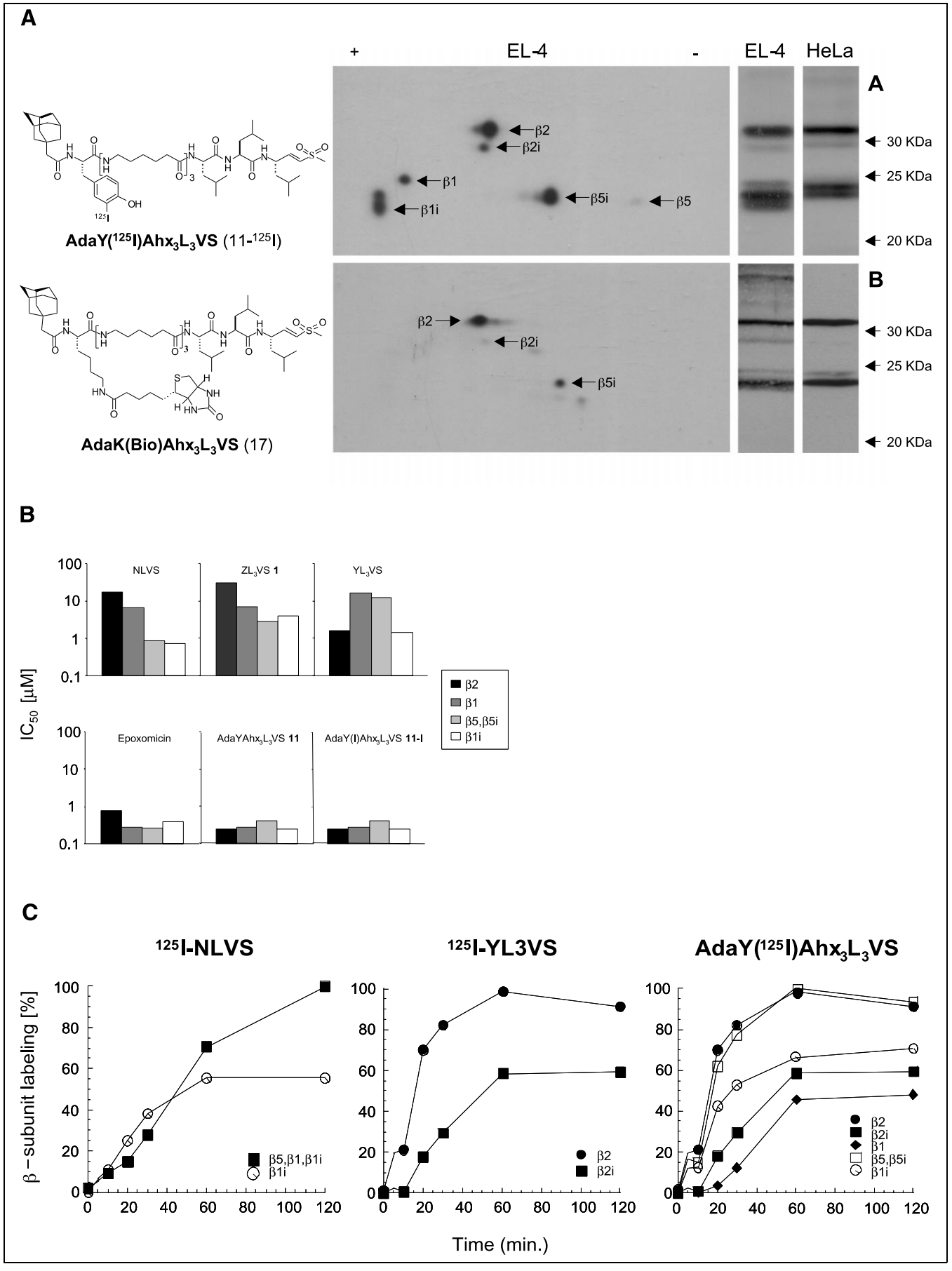
A
+
EL-4
-
EL-4
HeLa
A
β2
β2i
β1
β1i
β5i
β5
30 KDa
25 KDa
20 KDa
AdaY(125I)Ahx3L3VS (11-125I)
B
β2
β2i
β5i
30 KDa
25 KDa
20 KDa
AdaK(Bio)Ahx3L3VS (17)
B
IC50 [μM]
NLVS
ZL3VS 1
YL3VS
Epoxomicin
AdaYAhx3L3VS 11
AdaY(I)Ahx3L3VS 11-I
β2
β1
β5,β5i
β1i
C
125I-NLVS
125I-YL3VS
AdaY(125I)Ahx3L3VS
β-subunit labeling [%]
β5,β1,β1i
β1i
β2
β2i
β2
β2i
β1
β5,β5i
β1i
Time (min.)

Table 1
Potency of N-terminally extended peptide vinylsulfones for inhibition of the 20S proteasome activities[a]

Compounds	k_{obs}/[I] (M^{-1} s^{-1})		
	Chymotryptic-like activity	Trypsin-like activity	PGPH activity
(1) AdaAhx$_3$L$_3$VS **7**	8 200 ± 2 000 (0.05–0.01 μM)[b]	700 ± 180 (1–5 μM)	1 024 ± 350 (0.5–1 μM)
(2) AdaYAhx$_3$L$_3$VS **13**	11 500 ± 2 000 (0.05–0.1 μM)	240 ± 40 (1–5 μM)	604 ± 160 (1–2 μM)
(3) AdaK(Bio)Ahx$_3$L$_3$VS **17**	10 000 ± 1 500 (0.05–0.1 μM)	40 ± 13 (5–10 μM)	200 ± 30 (2–5 μM)
(7) ZAhx$_5$L$_3$VS **4**	3 300 ± 800 (0.2–0.5 μM)	85 ± 19 (10–20 μM)	102 ± 52 (2–5 μM)
(6) NLVS	4 500 ± 1 100 (0.1–0.2 μM)	4 ± 1 (50–250 μM)	14 ± 3 (25–50 μM)
(9) YL$_3$VS	70 ± 15 (5–10 μM)	174 ± 22 (5–10 μM)	8 ± 3 (10–50 μM)
(8) Epoxomicin	10 000 ± 2 000 (0.1–0.5 μM)	80 ± 22 (5–10 μM)	21 ± 7 (5–10 μM)

[a]See Section 5.
[b]Values in parentheses indicated the range of inhibitor concentration used.

In the next set of experiments, we examined labeling efficiency of AdaY(^{125}I)Ahx$_3$L$_3$VS **11**-^{125}I (Fig. 5). The choice of ^{125}I as label was made because of the ease of detection of this isotope by autoradiography. EL-4 lysates were treated with 0–30 μM ZL$_3$VS, NLVS, YL$_3$VS, epoxomicin, AdaYAhx$_3$L$_3$VS **11** and AdaY(I)Ahx$_3$L$_3$VS **11**-I, respectively, prior to labeling with **11**-^{125}I (Fig. 5B). Importantly, application of the new radiolabeled probe improved resolution (compare to for instance ^{125}I-NLVS) of the proteasomal subunits, with four of the six possible β-subunits clearly resolved. The different competitors could now be compared in a straightforward manner. As expected, NLVS and ZL$_3$VS inhibit labeling mainly of β5/β5i, whereas YL$_3$VS preferentially blocks labeling of β2/β2i. Of note, NLVS and YL$_3$VS inhibit at much higher concentrations than was observed in the reverse experiment (inhibition of labeling with ^{125}I-YL$_3$VS or ^{125}I-NLVS with **11** and **11**-I, see Fig. 4B). Both AdaYAhx$_3$L$_3$VS **11** and AdaY(I)Ahx$_3$L$_3$VS **11**-I compete for labeling of all subunits in a concentration range comparable to that for epoxomicin.

Two-dimensional (2D) SDS–PAGE analysis of EL-4 lysate labeled with AdaY(^{125}I)Ahx$_3$L$_3$VS **11**-^{125}I showed that most proteasomal subunits were labeled roughly equally well (Fig. 5A). With the possible exception of β5, all subunits are clearly visible, including β1, which is usually the most resistant towards active site labels. Note that this experiment shows labeling of an otherwise unfractionated cell extract; the selectivity of labeling is evident.

A similar experiment was carried out with AdaK(Bio)Ahx$_3$L$_3$VS **17**, followed by detection of labeled β-subunits by means of a streptavidin-horseradish peroxidase conjugate. The β2, β2i and β5i subunits are labeled, but labeling of β1 is less obvious (Fig. 5A). Although less efficient than the corresponding radiolabel (**11**-^{125}I), biotinylated proteasome inhibitor **17** readily allows detection of both constitutive and immunoproteasomal subunits.

Both AdaY(^{125}I)Ahx$_3$L$_3$VS **11**-^{125}I and AdaK(Bio)-Ahx$_3$L$_3$VS **17** label all three subunits of the constitutive proteasome in NIH-3T3 lysates (Fig. 5A). The mere introduction of the biotin moiety affects the pattern of labeling, showing again the effect of modifications at considerable distance from P1 on the β-subunits targeted.

The time-dependent labeling of EL-4 lysates with AdaY(^{125}I)Ahx$_3$L$_3$VS **11**-^{125}I was assayed next (Fig. 5C). Comparison with ^{125}I-NLVS and ^{125}I-YL$_3$VS revealed that all targeted subunits are modified at a comparable rate, with modification by AdaY(^{125}I)Ahx$_3$L$_3$VS **11**-^{125}I being possibly slightly faster (labeled bands are normalized with the most densely labeled band at 100%).

2.5. N-terminally extended peptide vinyl sulfones block hydrolysis of fluorogenic substrates

The inhibition of proteasome-mediated substrate hydrolysis with selected proteasome inhibitors was measured (Table 1). We performed our kinetic measurements not on crude EL-4 extracts, but rather on 20S proteasomes purified from rabbit muscle as a more convenient source from which large amounts of 20S proteasomes could be prepared [8]. This preparation also eliminates any confounding effects that might arise from the presence of β1i, β2i and β5i. Purified 20S proteasome was incubated with fluorogenic substrates (Suc-LLVY-AMC, to assay chymotryptic activity; Boc-LRR-AMC, to assay tryptic activity, and Z-LLE-βNA, to assay PGPH activity) for 5 min to establish the initial rate of hydrolysis. Subsequent inclusion of inhibitor allows the determination of the kinetic constants for inhibition. ZAhx$_5$L$_3$VS **4**, AdaAhx$_3$L$_3$VS **7** and AdaYAhx$_3$L$_3$VS **11**, as well as the affinity label AdaK(Bio)Ahx$_3$L$_3$VS **17**, were compared

←
Fig. 5. Development of a novel set of radio- and affinity probes. A: 1D and 2D gel analysis of EL-4 and HeLa cell lysates labeled with either AdaY(^{125}I)Ahx$_3$L$_3$VS **11**-^{125}I or AdaK(Bio)Ahx$_3$L$_3$VS **17**. B: Labeling of proteasomal β-subunits with AdaY(^{125}I)Ahx$_3$L$_3$VS **11**-^{125}I is efficiently blocked by AdaYAhx$_3$L$_3$VS **11**, AdaY(I)Ahx$_3$L$_3$VS **11**-I, epoxomicin, but not NLVS, YL$_3$VS and ZL$_3$VS. C: AdaY(^{125}I)Ahx$_3$L$_3$VS **11**-^{125}I, ^{125}I-YL$_3$VS and ^{125}I-NLVS display comparable rates in proteasomal β-subunit labeling. Labeled bands are normalized with the most densely labeled band at 100%.

with the standard inhibitors NLVS, YL_3VS and epoxomicin (Table 1). All four compounds **4**, **7**, **11** and **17** block the chymotryptic-like activity (hydrolysis of Suc-LLVY-AMC) with an efficiency comparable to that of NLVS and epoxomicin. With the exception of AdaK(Bio)Ahx_3L_3VS **17**, the same holds true for inhibition of hydrolysis of Boc-LRR-AMC when compared to YL_3VS. Apparently, β1 and β5 are less sensitive to the nature of the N-terminal extension than β2.

The inhibition of hydrolysis of fluorogenic peptides corroborates the efficient inhibition of labeling as described before. Both AdaAhx_3L_3VS **7** and AdaYAhx_3L_3VS **11** strongly inhibited the PGPH activity, to an extent similar or better than that of the PGPH-specific inhibitor Ac-GPFL-α′,β′-epoxyketone [22]. A comparison of absolute values for the published kinetic studies is complicated by the use of purified proteasomes from different sources and the use of different fluorogenic peptide substrates. In our assays we did not include strong detergents such as SDS, often added to activate latent 20S proteasomal activity. Nonetheless, the kinetic parameters we established for the inhibitors used here are in good agreement with the published values. The ability of N-terminally extended peptide vinyl sulfones to inhibit all three catalytically active β-subunits roughly equally well, combined with their stronger inhibitory properties (compared to NLVS, YL_3VS and epoxomicin), so far makes them unique. In comparison, peptide boronates display efficient inhibition of both chymotryptic and PGPH activities but considerably less inhibition of the tryptic-like activity [20].

The type of assay used here, although useful for a qualitative assessment of inhibition activity, does not allow comparison of absolute numbers obtained for the individual activities as a means to determine subunit specificity.

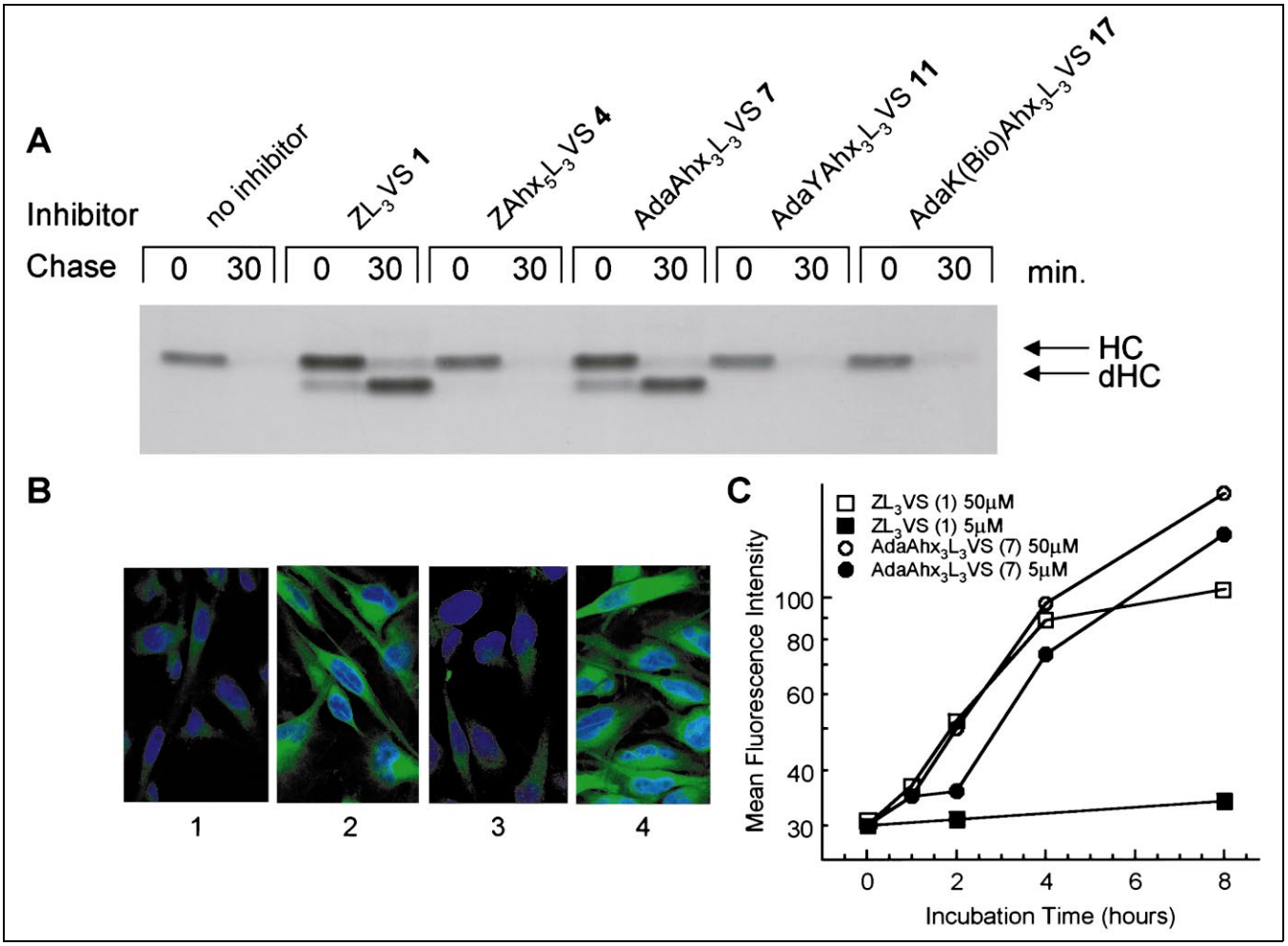

Fig. 6. AdaAhx_3L_3VS inhibits proteasomal proteolysis in living cells. A: Deglycosylated MHC I HC (HLA-A2) accumulates when proteasomal degradation is blocked in US11+ cells. ZL_3VS and AdaAhx_3L_3VS **7**, but not $ZAhx_5L_3VS$ **4**, AdaYAhx_3L_3VS **11** and AdaK(Bio)Ahx_3L_3VS **17** (50 μM final concentration), inhibit degradation of HC and allow accumulation of the deglycosylated HC intermediate. B: Cells were incubated with a solvent control (lane 1), ZL_3VS **1** (lane 2), $ZAhx_5L_3VS$ **4** (lane 3) and AdaAhx_3L_3VS **7** (lane 4) (50 μM inhibitor concentration) for 6 h, fixed, followed by blue nuclear staining of the DNA with DAPI (blue). Confocal laser scanning microscopy revealed that both ZL_3VS **1** and AdaAhx_3L_3VS **7** inhibit degradation of HLA-A2 with equal efficiency, as indicated by the levels of cytoplasmic green fluorescence. C: AdaAhx_3L_3VS **7** is a more potent inhibitor than ZL_3VS **1** on living cells. The proteasome inhibitors **1** and **7** were incubated at the indicated concentrations with U373 cells expressing US11 and GFP-A2. Accumulation of green fluorescence due to the presence of GFP-A2 in the cytosol was measured by flow cytometry.

The numbers reported for inhibition of the chymotryptic-like activity are almost always higher than those reported for the tryptic-like and PGPH activities, possibly due to different binding affinity and reactivity of the individual catalytic sites towards the fluorogenic substrates used. For instance, whereas fluorogenic assay of AdaYAhx$_3$L$_3$VS **11** would suggest β5 as the preferred target, direct labeling of HeLa lysate (see Fig. 5) revealed equal labeling of β2 and β5, with slightly less labeling of β1. A further caveat is the common use of purified 20S proteasome, which may not reflect cleavage behavior under physiological conditions. We therefore believe that labeling experiments of cell extracts, which contain the 26S proteasome, in combination with competition assays, to be the most accurate way to assess subunit specificity of potential proteasome inhibitors.

2.6. *AdaAhx$_3$L$_3$VS 7 blocks proteasome-mediated cytosolic proteolysis in living cells*

Inhibition of proteasomal activity in vivo with ZAhx$_5$L$_3$VS **4**, AdaAhx$_3$L$_3$VS **7**, AdaYAhx$_3$L$_3$VS **11** and AdaK(Bio)Ahx$_3$L$_3$VS **17** was compared with the known cell-permeable inhibitor ZL$_3$VS (Fig. 6). To this end we used an in vivo assay with cells that express the human cytomegalovirus US11 gene (US11+ cells). The US11 gene product accelerates degradation of MHC I heavy chain (HC) molecules by promoting their dislocation from the endoplasmic reticulum to the cytosol [33]. At this stage, the single *N*-glycan is removed from the HC, followed by proteasome-mediated degradation of the resulting polypeptide. In the presence of proteasome inhibitors, the deglycosylated class I HC accumulates transiently, as visualized by a pulse-chase experiment [33]. In the absence of proteasome inhibitor, degradation of class I HC is complete within the 30 min chase period (Fig. 6A). Addition of ZL$_3$VS allows recovery of deglycosylated HC. A similar result is obtained upon incubation of US11+ cells with AdaAhx$_3$L$_3$VS **7**, demonstrating its ability to cross the cell membrane and inhibit proteasomal function in living cells. Treatment with ZAhx$_5$L$_3$VS **4**, AdaYAhx$_3$L$_3$VS **11** or AdaK(Bio)Ahx$_3$L$_3$VS **17** did not result in any accumulation of deglycosylated class I HC (Fig. 6A), showing that these inhibitors are unable to cross the cell membrane. Inclusion of these inhibitors does not affect metabolic labeling and cellular integrity, demonstrating the absence of detergent-like properties.

In an independent experiment we examined the ability of ZAhx$_5$L$_3$VS **4** and AdaAhx$_3$L$_3$VS **7** to inhibit the breakdown of a different reporter, a green fluorescent protein (GFP)-tagged version of HLA-A2 (GFP-A2). When expressed in US11+ cells, the GFP-A2 HC is destroyed, and only background fluorescence is observed (D. Tortorella, E. Fiebiger and H.L. Ploegh, unpublished results). Inclusion of external ZL$_3$VS or AdaAhx$_3$L$_3$VS **7** resulted in a time-dependent increase of cytoplasmic fluorescence, consistent with the dislocation model proposed earlier (Fig. 6B). While AdaAhx$_3$L$_3$VS **7** allowed accumulation of GFP-A2, ZAhx$_5$L$_3$VS **4** did not. These experiments confirm the cell permeability of AdaAhx$_3$L$_3$VS **7**, but not ZAhx$_5$L$_3$VS **4**. When compared directly with ZL$_3$VS, we observed that in living cells AdaAhx$_3$L$_3$VS **7** is a far more (10-fold) potent inhibitor, as assayed by accumulation of the GFP-HLA-A2 reporter protein in the cytosol (Fig. 6C).

3. Discussion

Resolving the substrate specificity of the three individual catalytic activities in the constitutive proteasome, combined with that of their IFNγ-inducible counterparts, is a complicated task. An ideal tool to study proteasomal activity would be a set of molecules that mimic the natural substrate, and are equipped with a reporter entity. However, the nature of the proteasome dictates that any such molecule that resembles too closely the natural polypeptide substrate will most likely be processed by one of the catalytic β-subunits while reporting on the activity of a neighboring β-subunit, as we have observed for oligopeptide vinyl sulfones (B.M. Kessler and H.L. Ploegh, unpublished results). It is therefore not surprising that the considerable literature on peptide-based tools to study the proteasome, either fluorogenic substrates or inhibitors, mostly describe modified peptides limited in length to four amino acid residues. From these studies, selective fluorogenic substrates as well as inhibitors for the individual catalytic β-subunits have emerged. These are valuable tools to study the role of the individual β-subunits, both in vitro and in living cells. Longer substrate analogs need to be explored as inhibitors, on the premise that such compounds might better mimic the unfolded polypeptide that is the physiological substrate of the proteasome.

Here, we have presented a new class of substrate-like proteasome inhibitors that efficiently inhibit most proteasomal subunits. Our data suggest a considerable overlap between the individual catalytic activities of the proteasome when assayed with these compounds. The new proteasome inhibitors are based on a trileucine vinyl sulfone core as the C-terminal portion, a sequence previously shown to be capable of binding to the active site of the catalytic β-subunits. Extension has been accomplished by the introduction of a number of Ahx modules followed by different N-caps. We chose extension with Ahx spacers, as opposed to alkyl chains, to avoid complications that might arise from detergent-like properties of compounds with long alkyl chains. Reporter molecules, either radioiodinated tyrosine or biotinylated lysine, are placed near the N-terminus. The efficiency of both AdaY(^{125}I)Ahx$_3$L$_3$VS **11**-^{125}I and AdaK(Bio)Ahx$_3$L$_3$VS **17** to label proteasomal subunits indicates the resistance of this class of compounds to proteolytic cleavage. Labeled β-subunits can

of course be visualized only if both the C-terminal vinyl sulfone and the N-terminal label at a distance are retained.

The results presented here demonstrate the marked influence of extension, combined with the size of the N-terminal cap, on both activity and selectivity of proteasome inhibition. Regardless whether ^{125}I-YL$_3$VS or ^{125}I-NLVS is used as the active site label, the most potent inhibitors of active site labeling, ZAhx$_5$L$_3$VS **4**, AdaAhx$_3$L$_3$VS **7** and AdaYAhx$_3$L$_3$VS **11**, show a remarkably equal inhibition profile towards all proteasomal subunits assayed. This potent inhibition profile with little apparent discrimination for the individual β-subunits has, to our knowledge, not been demonstrated previously. Of interest are two literature examples describing comparable extended proteasome inhibitors. For instance, epoxomicin derivatives equipped with a biotin moiety through several Ahx residues were proven to be efficient affinity reagents for several, but not all, catalytic β-subunits [31,32]. Furthermore, two trileucine aldehyde molecules linked through polyethylene glycol spacers corresponding in size to lengths up to 25 amino acid residues have been shown to be potent proteasome inhibitors and inactivate predominantly the two trypsin-like and chymotrypsin-like activities in both β-rings simultaneously [34,35].

Analysis of substrate hydrolysis essentially confirmed the overall inhibition profile of the most potent inhibitors, although here ZAhx$_5$L$_3$VS **4** turns out to be 3–10-fold less active than AdaAhx$_3$L$_3$VS **7** and AdaYAhx$_3$L$_3$VS **11**. However, it should be noted that in the different assays different populations of proteasomes are used (either 26S for EL-4 cell extracts or rabbit 20S proteasomes for fluorogenic substrate assays).

The considerable overlap displayed by the individual catalytic β-subunits in recognizing our inhibitors corroborates by studies that address the proteasome-mediated digestion in vitro of entire proteins [6,7]. For instance, the 436 amino acid residue protein enolase I was digested with purified yeast 20S proteasome, as well as several mutant versions of 20S proteasomes in which individual catalytic β-subunits were genetically incapacitated. Several remarkable observations, indicating a high substrate redundancy between the three catalytic subunits, were made. Thus, although cleavage after acidic and basic residues was clearly attributed to the β1/Pre3 subunit and the β2/Pup1 subunit, respectively, activity of these subunits was by no means restricted to cleavage of sites uniquely displaying these amino acids. Furthermore, the complexity, number and average length (approximately eight residues) of the degradation products (>400 oligopeptides) did not vary drastically using either wild-type or mutant proteasomes (including a mutant in which both β1/Pre3 and β2/Pup1 were inactivated), indicating considerable overlap between the individual catalytically active proteasomal β-subunits. Similar observations were made in studies with mammalian proteasomes, in which β5, but not β1 and β2, were pharmacologically disabled by the covalent inhibitor NLVS [36]. Such overlap is not surprising, given the fact that proteasomes of the archaebacterium *Thermoplasma acidophilum*, composed of 14 identical α-subunits and 14 identical β-subunits, are obviously capable of processing polypeptides but must do with only a single type of catalytic β-subunit.

It is tempting to assume that more efficient proteasome inactivation can be obtained by simply extending the size of a given inhibitor. However, the steep loss of inhibition observed by replacement of the N-terminal Ada to Ac as in AcAhx$_3$L$_3$VS **13** and AcYAhx$_3$L$_3$VS **14** suggests a more complicated mode of action. Apparently, elements distal from the active site can strongly influence the inhibitory properties. Given the nature of the acetyl group, which can be regarded as a truncated Ahx residue (and therefore AcAhx$_3$L$_3$VS **13** as a truncated ZAhx$_5$L$_3$VS **4**), it seems likely that steric reasons (a different folding of the compound inside the proteolytic chamber), rather than chemical properties, account for the change in inhibitory activity.

Labeling and competition experiments with AdaY(^{125}I)Ahx$_3$L$_3$VS **11**-^{125}I confirmed the high binding activity and lack of discrimination between the individual catalytic β-subunits. Competition of labeling of β2 and β5/β5i with either YL$_3$VS or NLVS could only be accomplished at relatively high concentrations of inhibitor, whereas both AdaYAhx$_3$L$_3$VS **11** and AdaY(I)Ahx$_3$L$_3$VS **11**-I proved to be as efficient as epoxomicin in blocking radiolabeling. 2D analysis of EL-4 lysates revealed a remarkably equal distribution over five of the six catalytic β-subunits present, with the exception of β5. HeLa cells, expressing the constitutive proteasome, show equal labeling of β2 and β5, with a slightly lower intensity of β1. Interestingly, the same loss of subunit specificity was observed upon elongation of YL$_3$VS (with a preference for β2/β2i) with the AdaAhx$_3$ moiety. Although slightly less efficient than the corresponding AdaY(^{125}I)Ahx$_3$L$_3$VS, AdaAhx$_3$Y(^{125}I)L$_3$VS labeled all proteasomal subunits with almost equal intensity (data not shown).

The identification of AdaAhx$_3$L$_3$VS **7** as a powerful, general inhibitor of all proteasomal activities provides new tools for the study of the proteasome. First of all, AdaAhx$_3$L$_3$VS **7** blocks proteasome-mediated hydrolysis in living cells at least 10 times better than ZL$_3$VS. Furthermore, both AdaK(Bio)Ahx$_3$L$_3$VS **17** and especially AdaY(^{125}I)Ahx$_3$L$_3$VS **11**-^{125}I are potent, general proteasome labels.

In order to study the roles of the constitutive proteasome and the immunoproteasome, it would be of great interest to develop novel probes that can discriminate between the two species. In this respect, the emerging view is that differences between the constitutive proteasome and the immunoproteasome concern not only preferred cleavage sites [37] but also the length of the oligopeptide products. Immunoproteasomes produce N-terminally extended antigen precursors, favoring the generation of antigenic

peptides for MHC I presentation [38]. The extended peptide vinyl sulfones reported here, which can be modified at will using the safety catch strategy, may help in the generation of inhibitors that better discriminate between the constitutive proteasome and the immunoproteasome.

4. Significance

The 26S proteasome is involved in many important biological processes. It degrades most cytosolic proteins and generates antigenic peptides presented by MHC I molecules. The constitutive proteasome contains three individual catalytic activities, β1, β2 and β5, each of which occur twice in the inner 20S core responsible for proteolysis. Upon exposure to IFNγ, APCs assemble a new proteolytic particle, the immunoproteasome, in which the three catalytic β-subunits from the constitutive proteasome are replaced with three distinct, but highly homologous catalytic activities β1i, β2i and β5i, respectively.

The physiological role and substrate specificity of the individual catalytic β-subunits of the proteasome are widely studied. Based on preferred cleavage of fluorogenic peptide substrates, activities of the proteasome have been classified as 'chymotryptic-like' (β5), 'tryptic-like' (β2) and 'PGPH' (β1). Studies with protein substrates, however, indicate a far more complicated cleavage preference, with considerable overlap between the individual catalytic activities. We have generated a new set of peptide-based proteasome inhibitors extended significantly at the N-terminus when compared to the reported tri- and tetrapeptide-based inhibitors. Compared to these relatively small inhibitors, inhibition in vitro of the proteasome is greatly enhanced with our new compounds, while subunit specificity is largely obliterated. These results reflect the extensive overlap in specificity of the individual catalytic subunits as observed with in vitro protein degradation.

5. Materials and methods

5.1. General

Amino acid building blocks and peptide synthesis reagents were purchased from Advanced ChemTech, Peptides International, Novabiochem and American Bioanalytical (piperidine, diisopropylethylamine, trifluoroacetic acid). Adamantane-acetic acid, TIS and iodoacetonitrile were purchased from Aldrich, iodoacetonitrile was passed over a basic alumina plug prior to use. 4-Sulfamylbutyrylaminomethyl polystyrene resin was purchased from Novabiochem AG. Proteasome substrates (Suc-LLVY-AMC, Boc-LRR-AMC, Z-LLE-βNA) were purchased from Bachem. Epoxomicin was purchased from Affiniti. Iodo-gen was purchased from Pierce. Leucine vinyl sulfone, YL_3VS, NLVS and 4-hydroxy-3-nitrophenylacetyl-leucinyl-leucinyl-leucine vinyl sulfone (NPL_3VS) were prepared as reported [15,16]. HPLC-grade organic solvents DMF, dichloromethane, acetonitrile, NMP (American Bioanalytical) and ethyl acetate (Fisher) were used as received. Sep-pak C_{18} columns were purchased from Waters. SPPS was carried out using a 180° Variable Rate Shaker (Peptides International). Nuclear magnetic resonance (NMR) spectra were recorded on a Varian 500 MHz spectrometer, mass spectra were recorded on an electrospray LCZ liquid chromatography–mass spectrometry (LC–MS) instrument (Micromass). Preparative reverse phase HPLC purifications were carried out using a Waters PrepLC™ C_{18} column (250 mm × 40 mm) with a solvent gradient ranging from 30 to 95% acetonitrile in water containing 0.1% formic acid.

5.2. Synthesis of the novel proteasome inhibitors

Route A (compounds **1**–**17**): Fmoc-Leu safety catch resin (50–100 μmol), prepared from Fmoc-Leu-OH and 4-aminosulfonylbutyryl polystyrene resin according to the literature procedure [26], was elongated by standard Fmoc-based SPPS. In brief, cleavage of the Fmoc protective group was accomplished by treatment of the resin with 20% (v/v) piperidine in DMF. Peptide coupling steps were performed using a five-fold excess of the appropriate amino acid building block (respectively Fmoc-Leu-OH, Fmoc-6-Ahx-OH, adamantane-acetic acid, Fmoc-Lys-(ε-biotin)-OH, Fmoc-Dpr-(NHβ-Fmoc)-OH and Fmoc-Tyr-(OBu)-OH) which was pre-activated with PyBOP (five equivalents) and DiPEA (six equivalents) in DMF. Coupling efficiencies were monitored with the Kaiser test, and couplings were repeated when necessary. The obtained immobilized peptides were treated with iodoacetonitrile (50 equivalents) and DiPEA (10 equivalents) in NMP for 24 h under exclusion of light to afford activated safety catch resin, which was then reacted with leucine vinyl sulfone TFA salt (10 equivalents), in the presence of DiPEA (12 equivalents) in DMF for 4 days. The reaction mixture was diluted with ethyl acetate and extracted with 5% aqueous potassium hydrogen sulfate (three times). The organic layer was dried over $MgSO_4$, filtered and concentrated in vacuo. Removal of the *tert*-butyl protective group (TFA/TIS/H_2O 95/2.5/2.5 v/v, for compounds **9**–**12**, **15**, **16**) gave the crude peptides in 10–45% yield. Preparative reverse phase HPLC afforded peptides **1**–**17** in 5–30% yield in analytically pure form.

Method B (compounds **4**, **7**, **11**, **17**). Fmoc-Leu-Wang resin (0.5–1.0 mmol) was elongated using standard Fmoc-SPPS. Treatment of the immobilized peptides with TFA/TIS/H_2O 95/2.5/2.5 v/v and removal in vacuo of the solvents were followed by solution phase block coupling with leucine vinyl sulfone TFA salt (one equivalent) under the agency of HBTU (one equivalent) and DiPEA (2.2 equivalents) in DMF. After evaporation of the solvent the residue was dissolved in ethyl acetate. Precipitation of the product was accomplished by sonication for 2 min. The precipitate was filtered and washed with ethyl acetate, diethyl ether and hexanes to afford peptides **4**, **7**, **11**, **17** in 40–55% yield in 90–95% homogeneity, as judged by LC–MS and NMR analysis.

5.3. Selected analytical data

ZL_3VS **1**: MS: found 551.5 $(M+H)^+$. ^{1}H-NMR (DMSO-d6, 500 MHz): δ 8.01–7.82 (m, 3H), 7.41–7.30 (m, 4H), 7.27–7.21 (m, 1H), 6.66 (dd, 1H, *J* 4.5 and 15.5 Hz), 6.60 (d, 1H, *J* 15.5 Hz), 4.99 (s, 2H), 2.98 (s, 3H), 1.62–1.22 (m, 9H), 0.94–0.80 (m, 18H).

$ZAhxL_3VS$ **2**: MS: found 665.3 $(M+H)^+$. ^{1}H-NMR (DMSO-

d6, 500 MHz): δ 8.02–7.80 (m, 4H), 7.41–7.30 (m, 4H), 7.27–7.21 (m, 1H), 6.66 (dd, 1H, *J* 4.5 and 15.5 Hz), 6.60 (d, 1H, *J* 15.5 Hz), 5.00 (s, 2H), 3.01–2.93 (m, 2H), 2.98 (s, 3H), 2.16–2.04 (m, 2H), 1.64–1.18 (m, 15H), 0.94–0.80 (m, 18H).

ZAhx$_3$L$_3$VS **3**: MS: found 892.1 (M+H)$^+$. ^{1}H-NMR (DMSO-d6, 500 MHz): δ 8.00–7.94 (m, 4H), 7.76–7.70 (m, 2H), 7.40–7.29 (m, 4H), 7.28–7.22 (m, 1H), 6.60 (dd, 1H, *J* 5.0 and 15.0 Hz), 6.60 (d, 1H, *J* 15.5 Hz), 4.99 (s, 2H), 4.59–4.52 (m, 1H), 4.29–4.22 (m, 2H), 3.03–2.94 (m, 6H), 2.98 (s, 3H), 2.18–2.09 (m, 2H), 2.05–1.99 (m, 4H), 1.62–1.16 (m, 27H), 0.93–0.81 (m, 18H).

ZAhx$_5$L$_3$VS **4**: MS: found 1117.8 (M+H)$^+$. ^{1}H-NMR (DMSO-d6, 500 MHz): δ 7.99–7.92 (m, 4H), 7.76–7.70 (m, 4H), 7.39–7.28 (m, 4H), 7.26–7.21 (m, 1H), 6.55 (dd, 1H, *J* 5.0 and 15.0 Hz), 6.59 (d, 1H, *J* 15 Hz), 4.99 (s, 2H), 4.58–4.51 (m, 1H), 4.29–4.20 (m, 2H), 3.01–2.91 (m, 13H), 2.14–2.06 (m, 2H), 2.05–1.98 (m, 8H), 1.61–1.14 (m, 39H), 0.91–0.80 (m, 18H).

AdaL$_3$VS **5**: MS: found 594.2 (M+H)$^+$. ^{1}H-NMR (DMSO-d6, 500 MHz): δ 7.97 (d, 1H, *J* 8.5 Hz), 7.93 (d, 1H, *J* 8.5 Hz), 7.86 (d, 1H, *J* 7.5 Hz), 6.67 (dd, 1H, *J* 5.0 and 15.5 Hz), 6.59 (d, 1H, *J* 15.5 Hz), 4.57–4.50 (m, 1H), 4.30–4.21 (m, 2H), 3.98 (s, 3H), 1.91–1.86 (m, 2H), 1.66–1.32 (m, 24H), 0.90–0.79 (m, 18H).

AdaAhxL$_3$VS **6**: MS: found 707.6 (M+H)$^+$. ^{1}H-NMR (DMSO-d6, 500 MHz): δ 8.01–7.94 (m, 3H), 7.63 (t, 1H, *J* 5.5 Hz), 6.65 (dd, 1H, *J* 4.5 and 15.5 Hz), 6.59 (d, 1H, *J* 15.5 Hz), 4.58–4.50 (m, 1H), 4.28–4.19 (m, 2H), 3.00–2.94 (m, 2H), 2.98 (s, 3H), 2.14–2.05 (m, 2H), 1.89 (s, 2H), 1.66–1.19 (m, 30H), 0.91–0.79 (m, 18H).

AdaAhx$_3$L$_3$VS **7**: MS: found 934.0 (M+H)$^+$. ^{1}H-NMR (DMSO-d6, 500 MHz): δ 7.80–7.96 (m, 3H), 7.75–7.70 (m, 2H), 7.65 (t, 1H, *J* 5.0 Hz), 6.65 (dd, 1H, *J* 5.0 and 15.0 Hz), 6.59 (d, 1H, *J* 15.5 Hz), 4.58–4.50 (m, 1H), 4.29–4.20 (m, 2H), 3.01–2.96 (m, 9H), 2.15–2.05 (m, 1H), 2.03–1.99 (m, 4H), 1.89 (s, 2H), 1.66–1.14 (m, 42H), 0.90–0.79 (m, 18H).

AdaAhx$_5$L$_3$VS **8**: MS: found 1160.4 (M+H)$^+$. ^{1}H-NMR (DMSO-d6, 500 MHz): δ 7.98–7.92 (m, 3H), 7.76–7.68 (m, 4H), 7.64 (t, 1H, *J* 5.0 Hz), 6.65 (dd, 1H, *J* 5.0 and 15.0 Hz), 6.59 (d, 1H, *J* 15.0 Hz), 4.59–4.50 (m, 1H), 4.30–4.21 (m, 2H), 3.01–2.95 (m, 13H), 2.15–2.05 (m, 1H), 2.03–1.99 (m, 8H), 1.89 (s, 2H), 1.66–1.15 (m, 54H), 0.90–0.80 (m, 18H).

ZYAhx$_3$L$_3$VS **9**: MS: found 1054.4 (M+H)$^+$. ^{1}H-NMR (DMSO-d6, 500 MHz): δ 7.99–7.88 (m, 5H), 7.74–7.69 (m, 2H), 7.40–7.21 (m, 6H), 6.69–6.62 (m, 3H), 6.59 (d, 1H, *J* 15.0 Hz), 4.95 (d, 1H, *J* 12.5 Hz), 4.91 (d, 1H, *J* 12.5 Hz), 4.57–4.50 (m, 1H), 4.28–4.20 (m, 2H), 4.11–4.04 (m, 1H), 3.06–2.94 (m, 9H), 2.79 (dd, 1H, *J* 5.0 and 13.5 Hz), 2.61 (dd, 1H, *J* 10.0 and 13.5 Hz), 2.15–2.04 (m, 2H), 2.04–1.98 (m, 4H), 1.61–1.12 (m, 27H), 0.91–0.79 (m, 18H).

ZYAhx$_5$L$_3$VS **10**: MS: found 1280.2 (M+H)$^+$. ^{1}H-NMR (DMSO-d6, 500 MHz): δ 7.98–7.88 (m, 5H), 7.77–7.68 (m, 4H), 7.38–7.20 (m, 6H), 6.68–6.63 (m, 3H), 6.59 (d, 1H, *J* 15.5 Hz), 4.96 (d, 1H, *J* 12.5 Hz), 4.91 (d, 1H, *J* 12.5 Hz), 4.58–4.41 (m, 1H), 4.29–4.20 (m, 2H), 4.10–4.04 (m, 1H), 3.06–2.96 (m, 13H), 2.80 (dd, 1H, *J* 5.0 and 13.5 Hz), 2.61 (dd, 1H, *J* 10.0 and 13.5 Hz), 2.14–2.05 (m, 2H), 2.04–1.98 (m, 8H), 1.61–1.16 (m, 39H), 0.90–0.80 (m, 18H).

AdaYAhx$_3$L$_3$VS **11**: MS: found 1097.1 (M+H)$^+$. ^{1}H-NMR (DMSO-d6, 500 MHz): δ 8.12 (d, 1H, *J* 9.0 Hz), 7.98–7.92 (m, 3H), 7.85–7.80 (m, 2H), 7.75–7.68 (m, 2H), 6.99–7.97 (m, 2H), 6.67–6.58 (m, 4H), 4.58–4.50 (m, 1H), 4.41–4.35 (m, 1H), 4.28–4.20 (m, 2H), 3.05–2.95 (m, 9H), 2.81 (dd, 1H, *J* 5.0 and 13,5 Hz), 2.62 (dd, 1H, *J* 9.8 and 13.5 Hz), 2.14–2.04 (m, 2H), 2.02–1.96 (m, 4H), 1.80 (s, 2H), 1.60–1.24 (m, 42H), 0.91–0.80 (m, 18H).

AdaYAhx$_5$L$_3$VS **12**: MS: found 1323.2 (M+H)$^+$. ^{1}H-NMR (DMSO-d6, 500 MHz): δ 7.98–7.92 (m, 4H), 7.80 (t, 1H, *J* 5.5 Hz), 7.76–7.70 (m, 5H), 7.00–6.98 (m, 2H), 6.70–5.56 (m, 4H), 4.59–4.51 (m, 1H), 4.41–4.34 (m, 1H), 4.48–4.18 (m, 2H), 3.02–2.94 (m, 13H), 2.82 (dd, 1H, *J* 5.0 and 13,5 Hz), 2.63 (dd, 1H, *J* 10.0 and 13.5 Hz), 2.07–2.02 (m, 2H), 2.02–1.97 (m, 8H), 1.80 (s, 2H), 1.60–1.16 (m, 54H), 0.90–0.79 (m, 18H).

AcAhx$_3$L$_3$VS **13**: MS: found 799.6 (M+H)$^+$. ^{1}H-NMR (DMSO-d6, 500 MHz): δ 8.00 (d, 1H, *J* 8.5 Hz), 7.99–7.91 (m, 3H), 7.88 (t, 1H, *J* 5.5 Hz), 6.67 (dd, 1H, *J* 5.0 and 15.5 Hz), 6.59 (d, 1H, *J* 15.5 Hz), 4.58–4.51 (m, 1H), 4.28–4.19 (m, 2H), 3.01–2.91 (m, 9H), 2.14–2.05 (m, 2H), 2.03–1.97 (m, 4H), 1.75 (s, 3H), 1.61–1.12 (m, 27H), 0.89–0.79 (m, 18H).

AdaDpr(Ada)Ahx$_3$L$_3$VS **14**: MS: found 1196.0 (M+H)$^+$. ^{1}H-NMR (DMSO-d6, 500 MHz): δ 7.98–7.92 (m, 3H), 7.76–7.70 (m, 4H), 7.62 (t, 1H, *J* 5.5 Hz), 6.67 (dd, 1H, *J* 5.5 and 15.0 Hz), 6.59 (d, 1H, *J* 15.0 Hz), 4.58–4.51 (m, 1H), 4.29–4.20 (m, 3H), 3.25–3.19 (m, 1H), 3.03–2.92 (m, 10H), 2.13–2.05 (m, 2H), 2.03–1.97 (m, 4H), 1.88 (bs, 4H), 1.65–1.17 (m, 57H), 0.90–0.80 (m, 18H).

AcYAhx$_3$L$_3$VS **15**: MS: found 962.4 (M+H)$^+$. ^{1}H-NMR (DMSO-d6, 500 MHz): δ 8.00 (d, 1H, *J* 8.5 Hz), 7.98–7.91 (m, 4H), 7.88 (t, 1H, *J* 5.5 Hz), 7.74–7.69 (m, 2H), 6.91–6.88 (m, 2H), 6.68–6.55 (m, 4H), 4.58–4.51 (m, 1H), 4.35–4.28 (m, 1H), 4.28–4.19 (m, 2H), 3.02–2.91 (m, 9H), 2.77 (d, 1H, *J* 5.0 and 14.0 Hz), 2.59 (dd, 1H, *J* 9.5 and 13.5 Hz), 2.14–2.05 (m, 2H), 2.03–1.97 (m, 4H), 1.75 (s, 3H), 1.60–1.11 (m, 27H), 0.89–0.78 (m, 18H).

AdaDpr(Ada)YAhx$_3$L$_3$VS **16**: MS: found 1359.2 (M+H)$^+$. ^{1}H-NMR (DMSO-d6, 500 MHz): δ 7.97–7.91 (m, 3H), 7.86 (t, 1H, *J* 5.5 Hz), 7.79–7.21 (m, 5H), 7.67–7.62 (m, 1H), 6.95–6.93 (m, 2H), 6.68–6.55 (m, 4H), 4.58–4.50 (m, 1H), 4.33–4.28 (m, 1H), 4.27–4.21 (m, 2H), 3.25–3.19 (m, 1H), 3.03–2.92 (m, 10H), 2.76 (d, 1H, *J* 5.0 and 14.0 Hz), 2.57 (dd, 1H, *J* 9.5 and 13.5 Hz), 2.12–2.04 (m, 2H), 2.02–1.98 (m, 4H), 1.88 (s, 4H), 1.65–1.10 (m, 57H), 0.89–0.78 (m, 18H).

AdaK(Bio)Ahx$_3$L$_3$VS **17**: MS: found 1287.9 (M+H)$^+$. ^{1}H-NMR (DMSO-d6, 500 MHz): δ 8.11 (d, 1H, *J* 8.5 Hz), 7.99–7.93 (m, 2H), 7.84 (d, 1H, *J* 8.0 Hz), 7.74–7.68 (m, 2H), 7.07 (d, 1H, *J* 10.5 Hz), 6.68–6.56 (m, 3H), 4.57–4.50 (m, 1H), 4.31–4.10 (m, 4H), 4.00–3.94 (m, 1H), 3.08–2.94 (m, 16H), 2.14–2.08 (m, 2H), 2.04–1.98 (m, 4H), 1.88 (s, 2H), 1.62–1.16 (m, 54H), 0.91–0.80 (m, 18H).

5.4. Preparation of AdaY(I)Ahx$_3$L$_3$VS ***11*****-I**

AdaYAhx$_3$L$_3$VS **11** (0.01 mmol) was reacted for 15 min with sodium iodide (0.01 mmol) and chloramine T (0.01 mmol) in a 20/20/2 mixture of DMF/acetonitrile/phosphate buffer (pH 7.4). The reaction was quenched with aqueous $Na_2S_2O_5$ and extracted with ethyl acetate. After concentration in vacuo of the organic solvent, the mixture of starting material, mono- and bisiodinated compounds was purified by reverse phase HPLC to afford homogeneous AdaY(I)Ahx$_3$L$_3$VS **11**-I in 15% yield. MS: found 1222.4 (M+H)$^+$.

5.5. Preparation of ^{125}I-NLVS, ^{125}I-YL$_3$VS and AdaY(^{125}I)Ahx$_3$L$_3$VS

Radioiodination of the proteasome inhibitors was carried out

as follows. Iodo-gen (100 μg) was dissolved in phosphate buffer (50 mM, pH 7.4, 10 μl). Proteasome inhibitor (20 μg; NPL_3VS, YL_3VS or $AdaYAhx_3L_3VS$) in acetonitrile (30 μl) was added and the mixture was agitated for 2 min. $Na^{125}I$ (10 μl aqueous solution, 1 mCi) was added in the mixture agitated for 2 min. The radioiodinated proteasome inhibitor was separated using a Sep-pak C_{18} column. Free iodine was washed away with phosphate buffer pH 7.4 and the radiolabels ^{125}I-NLVS, ^{125}I-YL_3VS and $AdaY(^{125}I)Ahx_3L_3VS$ were eluted using acetonitrile. Fractions of 1 ml were collected and the fractions containing most radioactivity (typically $0.3–0.7\times10^6$ cpm/μl) were used for radiolabeling experiments.

5.6. Cell cultures and preparation of cell lysates

The mouse EL-4 cell line was cultured in RPMI and HeLa cells in Dulbecco's modified Eagle medium, both supplemented with 10% fetal calf serum, 1% glutamine and 1% penicillin/streptomycin. The US11+ U373 cell line [39] was transfected with a GFP-HLA-A2 fusion construct preceded by the K^b signal sequence. A detailed description of the generation of this cell line will be reported elsewhere. Preparation of cell lysates was performed as previously described [17,18]. In brief, cells were washed twice with cold phosphate-buffered saline, pelleted and lysed with one volume of glass beads (<106 microns, acid-washed; Sigma Chem. Co., St. Louis, MO, USA) and an equal volume of homogenization buffer (50 mM Tris pH 7.4, 1 mM dithiothreitol (DTT), 5 mM $MgCl_2$, 2 mM ATP and 250 mM sucrose). The cells were subjected to three rounds of vortexing for 1 min and cooled on ice for 30 s. Beads, membrane fractions, nuclei and cell debris were removed by centrifugation at 13 000 rpm for 30 min. The protein content was assayed by BCA protein quantification (Pierce).

5.7. Labeling of proteasomes and competition experiments

Labeled inhibitors (0.5×10^6 cpm) were added to 25 μg of cell lysates and incubated for 2 h at 37°C unless noted otherwise. Samples were quenched by adding 3× SDS sample buffer (1× final concentration), heated to 95°C for 3 min and analyzed by one-dimensional (1D) SDS–PAGE (12.5%) followed by autoradiography. For 2D, non-equilibrium pH gradient SDS–PAGE (NEPHGE), the samples were prepared by adding urea (8 M final concentration) and NEPHGE sample buffer with Pharmacia ampholite pH 3–10. 2D NEPHGE SDS–PAGE analysis was performed as described [18]. In labeling competition experiments, the compounds **1**–**17**, **11**-I, NLVS, YL_3VS and epoxomicin at 0.3, 1, 3, 10 and 30 μM final concentrations were added from acetonitrile stocks (3% maximal final concentration of acetonitrile) to 25 μg cell lysates and incubated for 30 min at room temperature prior to the addition of either ^{125}I-NLVS or ^{125}I-YL_3VS. After incubation for 2 h at 37°C, the samples were analyzed by 12.5% SDS–PAGE and autoradiography. Labeled polypeptide bands were quantified using an AlphaImager 2000 (Alpha Innotech Corporation).

5.8. Purification of 20S proteasome

Rabbit muscle 20S proteasome was purified as described previously [8].

5.9. Proteasome labeling with $AdaK(Bio)Ahx_3L_3VS$ **17**

Cell lysates (25 μg) were incubated with 3 μg $AdaK(Bio)$-Ahx_3L_3VS **17** for 2 h at 37°C, followed by addition of 3× SDS sample buffer (1× final concentration) for SDS–PAGE. For 2D NEPHGE SDS–PAGE, 30 μl of samples was mixed with 220 μl of rehydration solution (8 M urea, 2% CHAPS, 0.5% IPG buffer (Amersham Pharmacia Biotech) pH 3–10, bromophenol blue, 18 mM DTT) and subjected to first dimension isoelectric focussing using a IPGphor isoelectric focussing system (Amersham Pharmacia Biotech) and second dimension 12.5% SDS–PAGE.

5.10. In vivo inhibition of proteasome-mediated proteolysis

Pulse-chase analysis experiments were carried out following the literature procedure [39]. US11+ U373 cells were incubated with 50 μM inhibitor for 1 h prior to biochemical analysis.

5.11. Immunofluorescence assay

Immunofluorescence experiments were performed as reported [40] with minor modifications. US11/GFP-A2 U373 cells were allowed to attach to slides overnight before incubation with the respective inhibitors (50 μM final concentration) from a DMSO stock (DMSO was used as a solvent control). After fixation with 4% formaldehyde for 20 min at room temperature cellular DNA was stained with DAPI (Molecular Probes) according to the manufacturer's guidelines. Analysis of green fluorescence was performed with a Bio-RDA MRC1024 confocal microscope. For the quantitative analysis of the inhibition of proteasomal proteolysis in living cells, the inhibitors were incubated at different concentrations with US11/GFP-A2 U373 cells up to 8 h at 37°C. The accumulation of green fluorescence due to proteasome inhibition was measured by flow cytometry (FACSCalibur, Becton Dickinson).

5.12. Enzyme kinetics assay

Peptide substrates Suc-LLVY-AMC, Boc-LRR-AMC or Z-LLE-βNA (100 μM final concentration) were incubated with 20S proteasomes at 37°C in 50 mM Tris–HCl (pH 7.5), 1 mM DTT. After 10 min appropriate amounts of inhibitor were added from DMSO stock solutions (1% DMSO final concentration) and fluorescence of released 7-amino-4-methylcoumarin (excitation 380 nm, emission 460 nm) or 2-naphthylamine (excitation 342 nm, emission 425 nm) was measured continuously for 45 min. k_{obs} values were obtained by fitting the data to a non-linear least-squares fit equation for time-dependent or slow binding inhibition [41], $\text{fluorescence} = v_s t+[(v_0-v_s)/k_{obs}]\cdot[1-\exp(-k_{obs}t)]$, where v_0 is the initial velocity that decays over time to a final velocity, v_s, with a rate constant, k_{obs}. The $k_{obs}/[I]$ values given are an average of three to five independent experiments with at least two different inhibitor concentrations.

Acknowledgements

The authors thank Alfred Goldberg for critical reading of the manuscript and Rod Andrade for recording the

NMR spectra. This work is supported by NIH Grant 5 R37 AI33456 to H.L.P. B.M.K. is a recipient of a long-term fellowship from the Human Frontiers Science Program Organization. D.T. is a Charles King Trust Fellow. A.F.K. is supported by a fellowship from the Medical Foundation and by grants from NSBRI and NIGMS to Alfred L. Goldberg. E.F. is a recipient of an Erwin Schrödinger Scholarship from the FWF Austria. H.S.O. is financially supported by the Netherlands Organization for Scientific Research (NWO).

References

[1] O. Coux, K. Tanaka, A.L. Goldberg, Structure and functions of the 20S and 26S proteasomes, Annu. Rev. Biochem. 65 (1996) 801–847.
[2] W. Baumeister, J. Walz, F. Zühl, E. Seemüller, The proteasome paradigm of a self-compartmentalizing protease, Cell 92 (1998) 367–380.
[3] D. Voges, P. Zwickl, W. Baumeister, The 26S proteasome: a molecular machine designed for controlled proteolysis, Annu. Rev. Biochem. 68 (1999) 1015–1068.
[4] E. Pamer, P. Cresswell, Mechanisms of MHC class I-restricted antigen processing, Annu. Rev. Immunol. 16 (1998) 323–358.
[5] K.L. Rock, A.L. Goldberg, degradation of cell proteins and the generation of MHC class I-presented peptides, Annu. Rev. Immunol. 17 (1999) 739–779.
[6] A.K. Nussbaum, T.P. Dick, W. Keilholz, M. Schirle, S. Stevanovic, K. Dietz, W. Heinemeyer, M. Groll, D.H. Wolf, R. Huber, H.-G. Rammensee, H. Schild, Cleavage motifs of the yeast 20S proteasome β subunits deduced from digests of enolase 1, Proc. Natl. Acad. Sci. USA 95 (1998) 12504–12509.
[7] T.P. Dick, A.K. Nussbaum, M. Deeg, W. Heinemeyer, M. Groll, M. Schirle, W. Keilholz, S. Stevanovic, D.H. Wolf, R. Huber, H.-G. Rammensee, H. Schild, Contribution of proteasomal β-subunits to the cleavage of peptide substrates analyzed with yeast mutants, J. Biol. Chem. 273 (1998) 25637–25646.
[8] A.F. Kisselev, T.N. Akopian, K.M. Woo, A.L. Goldberg, The sizes of peptides generated from protein by mammalian 26 and 20S proteasomes, J. Biol. Chem. 274 (1999) 3363–3371.
[9] N.P.N. Emmerich, A.K. Nussbaum, S. Stevanovic, M. Priemer, R.E.M. Toes, H.G. Rammensee, H. Schild, The human 26S and 20S proteasomes generate overlapping but different sets of peptide fragments from a model protein substrate, J. Biol. Chem. 275 (2000) 21140–21148.
[10] D.H. Lee, A.L. Goldberg, Proteasome inhibitors: valuable new tools for cell biologists, Trends Cell Biol. 8 (1998) 297–403.
[11] J. Loewe, D. Stock, R. Jap, P. Zwickl, W. Baumeister, R. Huber, Crystal structure of the 20S proteasome from the Archaeon *T. acidophilum* at 3.4-Angstrom resolution, Science 268 (1995) 533–539.
[12] M. Groll, L. Ditzel, J. Lowe, M. Bochtler, H.D. Bartunik, R. Huber, Structure of 20S proteasome from yeast at 2.4 A resolution, Nature 386 (1997) 463–471.
[13] M. Groll, K.B. Kim, N. Kairies, R. Huber, C.M. Crews, Crystal structure of epoxomicin: 20S proteasome reveals a molecular basis for selectivity of α′,β′-epoxyketone proteasome inhibitors, J. Am. Chem. Soc. 122 (2000) 1237–1238.
[14] S. Wilk, M. Orlowski, Evidence that pituitary cation-sensitivity neutral endopeptidase is a multicatalytic protease complex, J. Neurochem. 40 (1983) 842–849.
[15] G. Fenteany, R.F. Standaert, W.S. Lane, S. Choi, E.J. Corey, S.L. Schreiber, Inhibition of proteasome activities and subunit-specific amino-terminal threonine modification by lactacystin, Science 268 (1995) 533–539.
[16] M. Hanada, K. Sugawara, K. Kaneta, S. Toda, Y. Nishiyama, K. Tomita, H. Yamamoto, M. Konishi, T. Oki, Epoxomicin, a new antitumor agent of microbial origin, J. Antibiot. 45 (1992) 1746–1752.
[17] M. Bogyo, J.S. McMaster, M. Gaczynska, D. Tortorella, A.L. Goldberg, H. Ploegh, Covalent modification of the active site threonine of proteasomal β subunits and the *Escherichia coli* homolog HslV by a new class of inhibitors, Proc. Natl. Acad. Sci. USA 94 (1997) 6629–6634.
[18] M. Bogyo, S. Shin, J.S. McMaster, H.L. Ploegh, Substrate binding and sequence preference of the proteasome revealed by active-site-directed affinity probes, Chem. Biol. 5 (1998) 307–320.
[19] K.L. Rock, C. Gramm, L. Rothstein, K. Clark, R. Stein, L. Dick, D. Hwang, A.L. Goldberg, Inhibitors of the proteasome block the degradation of most cell proteins and the generation of peptides presented on MHC class I molecules, Cell 78 (1994) 761–771.
[20] J. Adams, M. Behnke, S. Chen, A.A. Cruickshank, L.R. Dick, L. Grenier, J.M. Klunder, Y.-T. Ma, L. Plamondon, R.L. Stein, Potent and selective inhibitors of the proteasome: dipeptidyl boronic acids, Bioorg. Med. Chem. Lett. 8 (1998) 333–338.
[21] M. Elofsson, U. Splittgerber, J. Myung, R. Mohan, C.M. Crews, Towards subunit-specific proteasome inhibitors: synthesis and evaluation of peptide α′,β′-epoxyketones, Chem. Biol. 6 (1999) 811–822.
[22] J. Myung, K.B. Kim, K. Lindsten, N.P. Dantuma, C.M. Crews, Lack of proteasome active site allostery as revealed by subunit-specific inhibitors, Mol. Cell 7 (2001) 411–420.
[23] T. Nazif, M. Bogyo, Global analysis of proteasomal substrate specificity using positional-scanning libraries of covalent inhibitors, Proc. Natl. Acad. Sci. USA 98 (2001) 2967–2972.
[24] A.F. Kisselev, T.N. Akopian, V. Castillo, A.L. Goldberg, Proteasome active sites allosterically regulate each other, suggesting a cyclical bite-chew mechanism for protein breakdown, Mol. Cell 4 (1999) 395–402.
[25] H.S. Overkleeft, G.H. Renkema, J. Neele, P. Vianello, I.O. Hung, A. Strijland, A.M. van der Burg, G.-J. Koomen, U.K. Pandit, J.M.F.G. Aerts, Generation of specific deoxynojirimycin-type inhibitors of the non-lysosomal glucosylceramidase, J. Biol. Chem. 273 (1998) 26522–26527.
[26] H.S. Overkleeft, P.R. Bos, B.G. Hekking, E.J. Gordon, H.L. Ploegh, B.M. Kessler, Solid phase synthesis of peptide vinyl sulfone and peptide epoxyketone proteasome inhibitors, Tetrahedron Lett. 41 (2000) 6005–6009.
[27] B.J. Backes, J.A. Ellman, An alkanesulfonamide 'safety catch' linker for solid-phase synthesis, J. Org. Chem. 64 (1998) 2322–2330.
[28] G.W. Kenner, J.R. McDermot, R.C. Sheppard, Safety catch principle in solid phase peptide synthesis, J. Chem. Soc. Chem. Commun. 12 (1971) 636–637.
[29] B.J. Backes, J.L. Harris, F. Leonetti, C.S. Craik, J.A. Ellman, Synthesis of position-scanning libraries of fluorogenic peptide substrates to define the extended substrate specificity of plasmin and thrombin, Nat. Biotechnol. 18 (2000) 187–193.
[30] A. Graiu, M. Gaczynska, T. Akopian, C.F. Gramm, G. Fenteany, A.L. Goldberg, K.L. Rock, Lactacystin and clasto-lactacystin β-lactone modify multiple proteasome β subunits and inhibit intracellular protein degradation and major histocompatibility complex class I antigen presentation, J. Biol. Chem. 272 (1997) 13437–13445.
[31] M. Sin, K.B. Kim, M. Elofsson, L. Meng, H. Auth, B.H.B. Kwok, C.M. Crews, Total synthesis of the potent proteasome inhibitor epoxomicin: a useful tool for understanding proteasome biology, Bioorg. Med. Chem. Lett. 9 (1999) 2283–2288.
[32] K.B. Kim, J. Myung, N. Sin, C.M. Crews, Proteasome inhibition by the natural products epoxomicin and dihydroeponemycin: insights into specificity and potency, Bioorg. Med. Chem. Lett. 9 (1999) 3335–3340.
[33] E.J.H.J. Wiertz, T.R. Jones, L. Sun, M. Bogyo, H.J. Geuze, H.L. Ploegh, The human cytomegalovirus US11 gene product dislocates

MHC class I heavy chains from the endoplasmic reticulum to the cytosol, Cell 84 (1996) 769–779.
[34] G. Loidl, M. Groll, H.-J. Musiol, R. Huber, L. Moroder, Bivalency as a principle for proteasome inhibition, Proc. Natl. Acad. Sci. USA 96 (1999) 5418–5422.
[35] G. Loidl, H.-J. Musiol, M. Groll, R. Huber, L. Moroder, Synthesis of bivalent inhibitors of eukaryotic proteasomes, J. Peptide Sci. 6 (2000) 36–46.
[36] E.W. Wang, B.M. Kessler, A. Borodovsky, B.J. Cravatt, M. Bogyo, H.L. Ploegh, R. Glas, Integration of the ubiquitin-proteasome pathway with a cytosolic oligopeptidase activity, Proc. Natl. Acad. Sci. USA 97 (2000) 9990–9995.
[37] P.-M. Kloetzel, Antigen processing by the proteasome, Nat. Rev. 2 (2001) 179–187.
[38] P. Cascio, C. Hilton, A.F. Kisselev, K.L. Rock, A.L. Goldberg, 26S proteasomes and immunoproteasomes produce mainly N-extended versions of an antigenic peptide, EMBO J. 20 (2001) 2357–2366.
[39] A. Rehm, P. Stern, H.L. Ploegh, D. Tortorella, Signal peptide cleavage of a type I membrane protein, HCMV US11, is dependent on its membrane anchor, EMBO J. 20 (2001) 1573–1582.
[40] C. Driessen, R.A.R. Bryant, A.M. Lennon-Dumenil, J.A. Villadangos, P.W. Bryant, G.P. Shi, H.A. Chapman, H.L. Ploegh, Cathepsin S controls the trafficking and maturation of MHC class II molecules in dendritic cells, J. Cell Biol. 147 (1999) 775–790.
[41] J.F. Morrison, C.T. Walsh, The behavior and significance of slow-binding enzyme inhibitors, Adv. Enzym. Relat. Areas Mol. Biol. 61 (1988) 201–301.